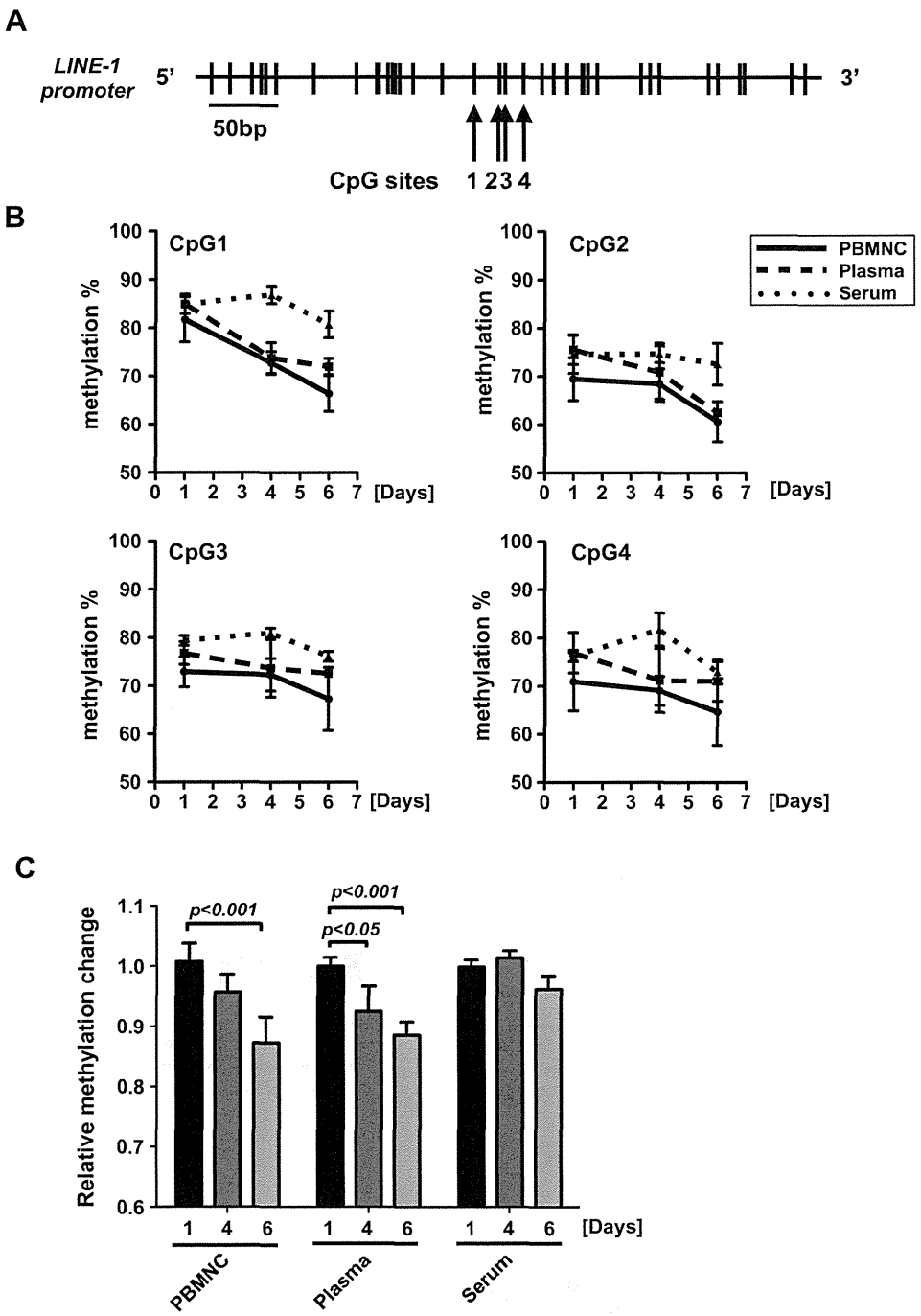

Fig. 2. *LINE-1* promoter CpG methylation status in a MDS patient treated with hypomethylating agent can be measured by using circulating DNAs. (A) Schematic representation of the *LINE-1* promoter CpG sites (GenBank; X58075, nucleotide position 108–520, complementary strand). Four CpG sites (1–4) were selected to measure cytosine methylation status by bisulfite pyrosequencing. (B) Peripheral blood was obtained from MDS UPN2 during the first azacitidine treatment cycle at days 1, 4, and 6. DNAs were prepared from plasma, serum, and PBMNC, and the methylation percentage of the four sites (CpG1–4) was quantitated by pyrosequencing analysis. The percentage of the methylation generally decreased after treatment with azacitidine. (C) The changing ratio of the methylation of all four sites was calculated using DNAs from PBMNC, plasma and serum, and the mean changing ratio was indicated in the bar graphs with the mean standard deviation (S.D.). The *p*-value was also indicated if the differences were significant.

plasma at day 4. In PBMNC, the tendency toward a decrease of the methylation ratio can be seen also at day 4, but was not significant. These data suggest that circulating DNA from plasma can be used for global methylation analysis with analysis of the *LINE-1* promoter as an alternative strategy using MNC in peripheral blood and/or BM.

3.3. Longer follow up of the global methylation status after treatment with a demethylating agent using plasma and serum circulating DNAs

Almost the same analysis was performed using peripheral blood samples from UPN4. PB was harvested 7 and 5 times during azacitidine treatment cycles 1 and 2 (Fig. 3A) and analyzed. The global

methylation ratio at the four CpG sites of the *LINE-1* elements generally decreased after starting treatment until day 9, and then increased again until the next treatment was started (days 12–28). To determine which samples of DNA were suitable for detection of the changing ratio after administration of azacitidine, the average methylation percentage of those four CpG sites was calculated using the data from days 1 to 9 in the first azacitidine course (Fig. 3B). In this assay, all DNA samples from PBMNC, plasma, and serum could detect the significant change of methylation status after azacitidine treatment. In particular, in this assay, plasma circulating DNA could detect the change much earlier at day 3 than DNA from PBMNC and serum. These data suggest that repeated sample collection from MDS patients can provide more accurate information about methylation status, and the methylation ratio of the *LINE-1* elements can be measured by using DNA circulating in the peripheral blood. Furthermore, taken together with the data of DNA concentration as shown in Fig. 1C, it is suggested that the DNA in plasma may be much more sensitive for detecting the change of methylation status in the blast cells in MDS patients.

3.4. Detection of genetic mutation using peripheral blood circulating DNAs

To test whether circulating DNAs can also be used for the detection of genetic mutations in MDS cells, mutation analysis was performed using plasma and serum circulating DNAs. BM cells from UPN1, showing 4q uni-parental disomy (UPD) by a SNP array (Fig. 4A), were utilized for genetic mutation analysis for the *TET2* gene. A non-sense point mutation of the *TET2* gene in exon 6, resulting in C-terminus truncation at the cysteine rich domain (CRD), was confirmed (Fig. 4B and C). Next, we performed pyrosequencing analysis to show the existence ratio of the *TET2* mutation

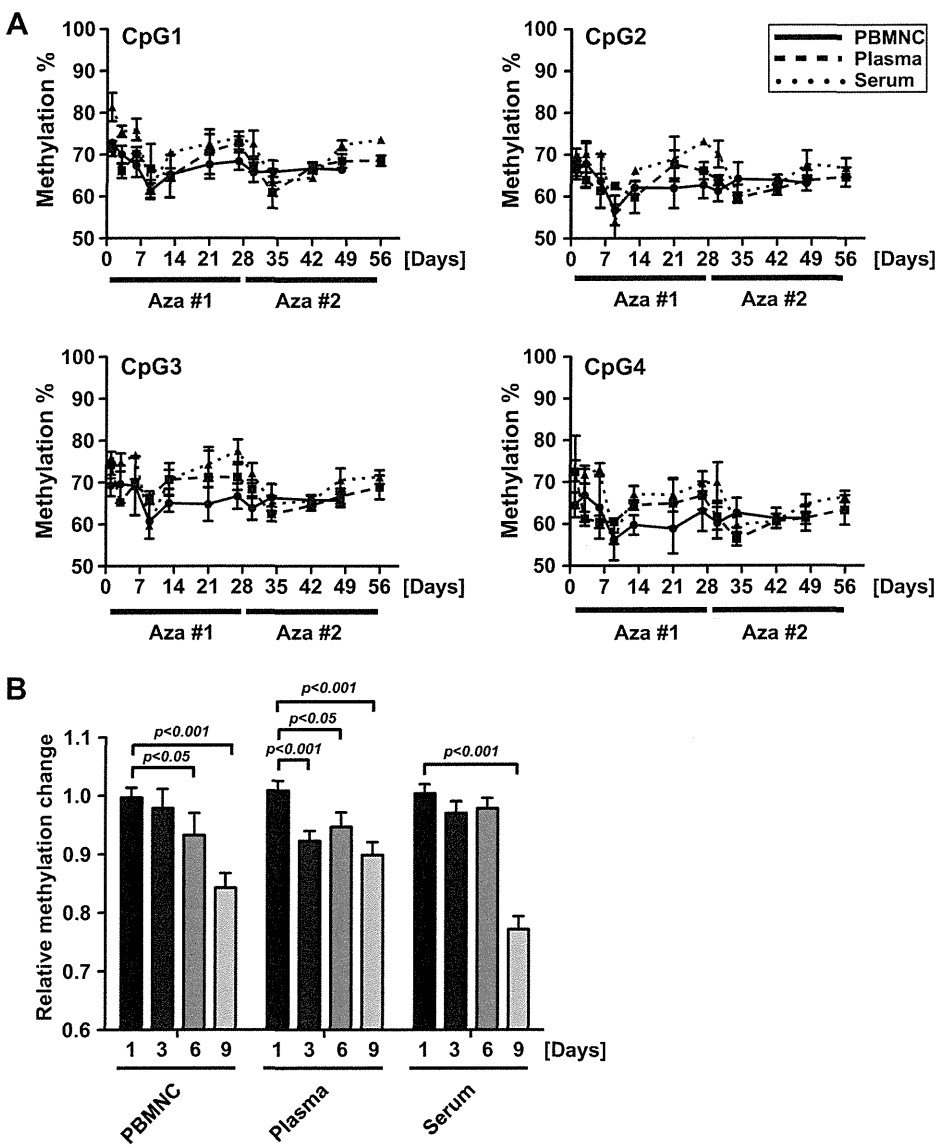

Fig. 3. A longer follow up of the *LINE-1* promoter CpG methylation status in an MDS patient treated with a hypomethylating agent using circulating DNAs. (A) Peripheral blood was obtained from MDS UPN4 during the first (#1) and the second (#2) azacitidine treatment cycle as indicated. DNAs were prepared from plasma, serum, and PBMNC, and the methylation percentage of the four sites (CpG1–4) was quantitated as analyzed in Fig. 2. Note that the methylation percentage was generally decreased until day 9, and the ratio was reversed until the next azacitidine treatment was started. (B) The mean changing ratio of the methylation of all four sites was calculated using DNAs from PBMNC, plasma, and serum, as analyzed in Fig. 2C.

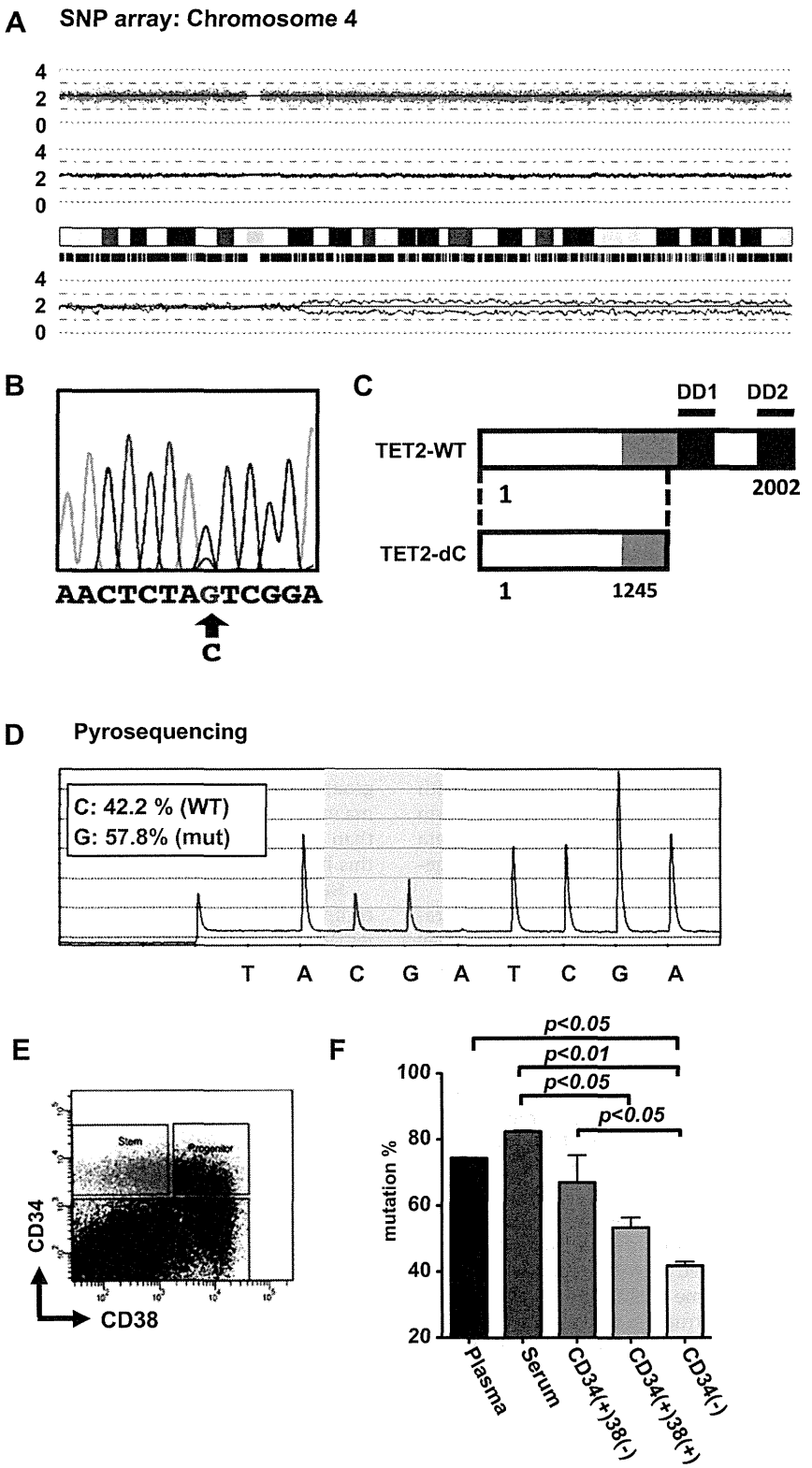

Fig. 4. Detection of the genetic mutations in an MDS patient using peripheral blood circulating DNAs. (A) SNP array analysis of UPN1. The DNA copy numbers were indicated on the green and red lines. UPD was observed in chromosome 4q. (B) Non-sense point mutation in the *TET2* gene exon 6, from TAC (tyrosine) to TAG (stop), was confirmed by the dye-terminator method. (C) Functional domains of wild-type TET2 and the putative C-terminally truncated TET2 protein (TET2-dC) in UPN1. CRD: cysteine rich domain, DD: dioxygenase domain. (D) Pyrosequencing analysis for the mutated region of the *TET2* gene using BM cells. The existence percentage of the wild-type (blue) and mutated (red) nucleotide was calculated by analyzing software. (E) BM cells of UPN1 were sorted into three subpopulations: CD34+/CD38− (stem), CD34+/CD38+(progenitor), and CD34− (others). (F) The existence ratio of the *TET2* mutation in each DNA prepared from circulating DNA (plasma and serum) and BM cell subpopulations (CD34+/CD38−, CD34+/CD38+, and CD34−).

using genomic DNA from whole BM cells of this patient. This mutation was detected by this assay indicating 57.8% of mutated clones. Since the mutation can be observed in both alleles in one cell (UPD), it was suggested that the wild type sequence came from the normal component of the patient.

To confirm whether the *TET2* mutation can also be detected in circulating DNA, and if so, whether the existing ratio of the mutation in circulating DNAs is much higher than that in components of BM cells, especially in stem cell population, three sorted BM cell populations (stem: CD34+/38−, progenitors: CD34+/38+, and others: CD34−) were utilized for the *TET2* mutation analysis using the pyrosequencing strategy. BM and peripheral blood aspiration from this patient were carried out in the same day. DNAs from plasma, serum, and the three populations of BM cells (Fig. 4E) were prepared, and pyrosequencing analysis was performed to confirm the existence ratio of the mutated *TET2* gene. The result was that the existence ratio of the mutants was significantly higher in serum and plasma than that in CD34-negative BM cells (Fig. 4F). These results indicated that circulating DNAs from plasma and serum can be used for the detection of genetic mutations in MDS cells. Furthermore, these data also suggest that plasma and serum DNA may likely come from the MDS clones distributed in these three populations, especially in CD34+/38− population, which might be relatively more fragile than normal cells. Further investigation is required to prove this hypothesis.

4. Discussion

The aim of this study was to check whether peripheral blood circulating DNA is useful for the detection of disease specific genetic and epigenetic changes in patients with MDS. Because MDS usually shows relatively slow disease progression compared with acute leukemia, patients and clinicians tend to hesitate to perform BM aspiration repeatedly to estimate the disease status. Our data suggest that plasma and serum DNAs are able to be used for the genetic and epigenetic assays instead of BM cells.

Interestingly, our data suggest that the plasma DNA concentration tends to reflect BM blast counts (Fig. 1C). This finding may indicate that the PB circulating DNA may come from relatively fragile MDS cells rather than normal cells. If so, there is a possibility that abnormal DNAs from the MDS clone may be much more enriched in the circulating DNA compared with DNAs from BM or PBMNC. This hypothesis may also explain two of our results: (1) the methylation status can be decreased more rapidly in plasma DNA than in PBMNC, as shown in Figs. 2C and 3B, (2) the existence ratio of the genetic mutation in plasma and serum DNA is relatively higher than that in the BM cells. A large number of patients are needed to confirm this phenomenon.

As shown in Fig. 1C, a higher concentration of digested DNA fragments, especially the accumulation of DNA fragments from mono-nucleosomes, can be observed in MDS patients who may have a relatively higher tumor volume in BM. Since the fragmentation of the DNA in the chromatin structure can occur through the enzymatic activity of deoxyribo-nuclease I (DNase I), a higher degree of enzymatic activity in plasma may serve as a biomarker that shows disease activity in MDS. Interestingly, further digestion of DNA fragments from one nucleosome structure (~200 bp) could be observed in UPN1 (Fig. 1C). This fragmentation could not be observed when we used the plasma sample after several freeze and thaw treatments (data not shown). This may indicate that some other DNase activity in specific patients correlates with this phenomenon. Further investigation is needed.

In our experiments, the plasma circulating DNA concentration of MDS patients was much higher than that in serum. An explanation for this phenomenon may be that many DNA fragments can be absorbed into blood clots after collection into sample tubes. The difference between the DNA concentrations in plasma and serum may correlate with the phenomenon that plasma DNA, compared with serum DNA, tends to more effectively detect the epigenetic changes in MDS cells (Figs. 2 and 3). These findings indicate that circulating DNA from plasma is better suited for epigenetic analysis than that from serum in MDS patients.

For detection of the CpG methylation status of specific gene promoters, we analyzed the methylation status of the $p15^{INK4B}$ promoter, known to be one of the hypermethylated genes in MDS patients [4,17]. Unfortunately, the result did not seem to be accurate with relatively varied data among the repeated experiments, even when using plasma DNA and nested PCR technique (data not shown). One possibility is that the DNA concentration was not sufficient for the bisulfite sequencing analysis. In contrast, the result of the *LINE-1* methylation (Figs. 2 and 3) was much more reliable compared with the analysis for the $p15^{INK4B}$ gene, because of the sufficient number of DNA copies for the *LINE-1* promoter: ~85,000 copies for *LINE-1* versus only two copies for the $p15^{INK4B}$ gene in one cell. From this standpoint, DNA methylation analysis focusing on the *LINE-1* promoter using plasma circulating DNA may be a good strategy to confirm the global methylation status in MDS patients.

Interestingly, an experiment for UPN4 indicated that the decreasing ratio of DNA methylation of the *LINE-1* promoter after treatment with azacitidine was detected much earlier when using plasma DNA (Figs. 2C, day 4, and 3B, day 3) than when using PBMNC (Figs. 2C and 3B, day 6). Since DNMTi are incorporated into DNA (and RNA) during cell division, MDS/AML cells that have a more rapid cell division cycle compared with intact cells may be affected more quickly by DNMTi in BM. Furthermore, MDS clones have a more fragile character resulting from "dysplastic" backgrounds. Taking this into consideration, circulating DNA from plasma may better reflect the DNA that comes from MDS clones in BM than from intact cells. Further investigation is required to prove this hypothesis.

Harvesting PB is painless, and is a safer and easier procedure compared with obtaining BM cells. Preparing plasma is much easier than preparing PBMNC, and plasma can very easily be stored in tubes in the freezer. Utilization of plasma circulating DNA for MDS patients may provide a new way to analyze the serial genetic/epigenetic changes that are integral to an understanding of MDS pathogenesis and their disease condition.

Acknowledgments

This work was supported by Grants-in-Aid from the Ministry of Health, Labor and Welfare, and the Ministry of Education, Culture, Sports, Science and Technology, Japan. We thank Dr. Seishi Ogawa and Dr. Masashi Sanada for performing the SNP array analysis. We thank Chika Wakamatsu, Eriko Ushida, Yukie Konishi, Mari Otsuka, Manami Kira, Mirei Okamoto, and Rie Kojima for valuable laboratory assistance.

References

[1] M.J. Walter, L. Ding, D. Shen, J. Shao, M. Grillot, M. McLellan, R. Fulton, H. Schmidt, J. Kalicki-Veizer, M. O'Laughlin, C. Kandoth, J. Baty, P. Westervelt, J.F. DiPersio, E.R. Mardis, R.K. Wilson, T.J. Ley, T.A. Graubert, Recurrent DNMT3A mutations in patients with myelodysplastic syndromes, Leukemia 25 (2011) 1153–1158.

[2] T. Ernst, A.J. Chase, J. Score, C.E. Hidalgo-Curtis, et al., Inactivating mutations of the histone methyltransferase gene EZH2 in myeloid disorders, Nat. Genet. 42 (2010) 722–726.

[3] K. Yoshida, M. Sanada, Y. Shiraishi, et al., Frequent pathway mutations of splicing machinery in myelodysplasia, Nature 478 (2011) 64–69.

[4] M. Kim, B. Oh, S.Y. Kim, et al., P15INK4b methylation correlates with thrombocytopenia, blast percentage, and survival in myelodysplastic

syndromes in a dose dependent manner: quantitation using pyrosequencing study, Leuk. Res. 34 (2010) 718–722.
[5] J. Lin, Y.L. Wang, J. Qian, et al., Aberrant methylation of DNA-damage-inducible transcript 3 promoter is a common event in patients with myelodysplastic syndrome, Leuk. Res. 34 (2010) 991–994.
[6] L. Shen, H. Kantarjian, Y. Guo, et al., DNA methylation predicts survival and response to therapy in patients with myelodysplastic syndromes, J. Clin. Oncol. 28 (2010) 605–613.
[7] G. Egger, G. Liang, A. Aparicio, P.A. Jones, Epigenetics in human disease and prospects for epigenetic therapy, Nature 429 (2004) 457–463.
[8] G. Garcia-Manero, P. Fenaux, Hypomethylating agents and other novel strategies in myelodysplastic syndromes, J. Clin. Oncol. 29 (2011) 516–523.
[9] H. Schwarzenbach, D.S. Hoon, K. Pantel, Cell-free nucleic acids as biomarkers in cancer patients, Nat. Rev. Cancer 11 (2011) 426–437.
[10] D. Allen, A. Butt, D. Cahill, M. Wheeler, R. Popert, R. Swaminathan, Role of cell-free plasma DNA as a diagnostic marker for prostate cancer, Ann. NY Acad. Sci. 1022 (2004) 76–80.
[11] E. Goto, A. Tomita, F. Hayakawa, A. Atsumi, H. Kiyoi, T. Naoe, Missense mutations in PML-RARA critical for the lack of responsiveness to arsenic trioxide treatment, Blood 118 (2011) 1600–1609.
[12] F. Ohka, A. Natsume, K. Motomura, et al., The global DNA methylation surrogate LINE-1 methylation is correlated with MGMT promoter methylation and is a better prognostic factor for glioma, PLoS ONE 6 (2011) e23332.
[13] M. Sanada, T. Suzuki, L.Y. Shih, et al., Gain-of-function of mutated C-CBL tumour suppressor in myeloid neoplasms, Nature 460 (2009) 904–908.
[14] A. Abe, Y. Minami, F. Hayakawa, et al., Retention but significant reduction of BCR-ABL transcript in hematopoietic stem cells in chronic myelogenous leukemia after imatinib therapy, Int. J. Hematol. 88 (2008) 471–475.
[15] A.P. Wolffe, Transcriptional activation. Switched-on chromatin, Curr. Biol. 4 (1994) 525–528.
[16] K. Balassiano, S. Lima, M. Jenab, et al., Aberrant DNA methylation of cancer-associated genes in gastric cancer in the European Prospective Investigation into Cancer and Nutrition (EPIC-EURGAST), Cancer Lett. 311 (2011) 85–95.
[17] T. Uchida, T. Kinoshita, H. Nagai, et al., Hypermethylation of the p15INK4B gene in myelodysplastic syndromes, Blood 90 (1997) 1403–1409.

Favorable outcome of patients who have 13q deletion: a suggestion for revision of the WHO 'MDS-U' designation

Kohei Hosokawa,[1] Takamasa Katagiri,[1,2] Naomi Sugimori,[1] Ken Ishiyama,[1,3] Yumi Sasaki,[1] Yu Seiki,[1] Aiko Sato-Otsubo,[4] Masashi Sanada,[4] Seishi Ogawa,[4] and Shinji Nakao[1]

[1]Cellular Transplantation Biology, Kanazawa University Graduate School of Medical Science, Kanazawa; [2]Clinical Laboratory Science, Kanazawa University Graduate School of Medical Science, Kanazawa; [3]Tokyo Metropolitan Ohtsuka Hospital, Department of Internal Medicine, Toshima; and [4]Cancer Genomics Project, Graduate School of Medicine, University of Tokyo, Tokyo, Japan

ABSTRACT

To characterize bone marrow failure with del(13q), we reviewed clinical records of 22 bone marrow failure patients possessing del(13q) alone or del(13q) plus other abnormalities. All del(13q) patients were diagnosed with myelodysplastic syndrome-unclassified due to the absence of apparent dysplasia. Elevated glycosylphosphatidylinositol-anchored protein-deficient blood cell percentages were detected in all 16 with del(13q) alone and 3 of 6 (50%) patients with del(13q) plus other abnormalities. All 14 patients with del(13q) alone and 2 of 5 (40%) patients with del(13q) plus other abnormalities responded to immunosuppressive therapy with 10-year overall survival rates of 83% and 67%, respectively. Only 2 patients who had abnormalities in addition to the del(13q) abnormality developed acute myeloid leukemia. Given that myelodysplastic syndrome-unclassified with del(13q) is a benign bone marrow failure subset characterized by good response to immunosuppressive therapy and a high prevalence of increased glycosylphosphatidylinositol-anchored protein-deficient cells, del(13q) should not be considered an intermediate-risk chromosomal abnormality.

Key words: glycosylphosphatidylinositol-anchored protein-deficient, cells, bone marrow failure, 13q deletion, immunosuppressive therapy.

Citation: Hosokawa K, Katagiri T, Sugimori N, Ishiyama K, Sasaki Y, Seiki Y, Sato-Otsubo A, Sanada M, Ogawa S, and Nakao S. Favorable outcome of patients who have 13q deletion: a suggestion for revision of the WHO 'MDS-U' designation. Haematologica 2012;97(12):1845-1849. doi:10.3324/haematol.2011.061127

Introduction

Numerical karyotypic abnormalities such as -7/del(7q) and del(13q) are occasionally seen in patients with bone marrow (BM) failure who do not exhibit typical signs of myelodysplasia. The 2008 World Health Organization (WHO) criteria defined this subset of BM failure as myelodysplastic syndrome-unclassified (MDS-U) because patient progression to leukemia was still possible. However, no large patient study has been conducted to explore an association between del(13q) and pre-leukemia.[1] Several anecdotal reports have shown that BM failure patients with del(13q) responded to immunosuppressive therapy (IST) and had a favorable prognosis.[2,3] However, the incidence of BM failure with del(13q) and its relationship with immune pathophysiology of BM failure remain unclear.

Several studies have identified the presence of small populations of glycosylphosphatidylinositol-anchored protein-deficient (GPI-AP$^-$) blood cells as a significant factor predicting a good response to IST in patients with aplastic anemia (AA) and low-risk myelodysplastic syndromes (MDS).[4,5] Immune mechanisms are, therefore, thought to be involved in the increase in the GPI-AP$^-$ cells in this type of BM failure, though the exact mechanisms responsible for the increase in the GPI-AP$^-$cells remain unknown. Given that BM failure with del(13q) is likely to respond to IST, this type of BM failure may be associated with the presence of small populations of GPI-AP$^-$ cells. It is essential to precisely characterize BM failure with del(13q) because the present WHO definition of an intermediate-risk abnormality may lead to inappropriate treatment of potentially benign BM failure with hypomethylating agents or allogeneic stem cell transplants from unrelated donors. To address this issue, the present study analyzed clinical and genetic features of 22 BM failure patients possessing del(13q) by comparing them to BM failure patients with a normal karyotype.

Design and Methods

Study subjects

Clinical records were analyzed for 1,228 BM failure patients: 733 with aplastic anemia (AA), 495 with low-risk MDS, including 286 with refractory cytopenia with unilineage dysplasia (RCUD), 149 with

The online version of this article has a Supplementary Appendix.

Acknowledgments: the authors would like to thank Rie Ohmi and Kenichi Takemoto for excellent technical assistance, and Yasuhiko Yamamoto for excellent cell sorting technical support. We also thank the doctors who contributed patients to this study: Mitsufumi Nishio, Ryosuke Yamamura, Yoshiko Okikawa, Takeaki Tomoyose, Takuya Machida, Hiroshi Kanashima, Masahiro Manabe, Yukiyoshi Moriuchi, Takashi Nakaike, Yutaka Imamura, Kenji Shinohara, Taro Masunari, Akio Maeda, Hirokazu Okumura, Kazuyuki Shigeno, Masayuki Kikukawa, Hidemi Ogura, Tadashi Nagai, Hidetaka Niitsu and Senji Kasahara.
Funding: this study was supported by grants awarded to SN.
Manuscript received on December 23, 2011. Revised version arrived on May 6, 2012. Manuscript accepted on June 7, 2012.
Correspondence: Shinji Nakao, MD, PhD, Cellular Transplantation Biology, Kanazawa University Graduate School of Medical Science, 13-1 Takaramachi, Kanazawa, Ishikawa 920-8640, Japan. Phone: international +81.76.2652274. Fax: international +81.76.2344252.
E-mail: snakao8205@staff.kanazawa-u.ac.jp

refractory cytopenia with multilineage dysplasia (RCMD) and 60 with MDS-U, whose blood samples were sent to our laboratory between May 1999 and July 2010 for screening of GPI-AP$^-$ granulocytes and erythrocytes. BM smear slides were reviewed by 2 independent hematologists. BM cellularity was defined as the percentage of BM volume occupied by hematopoietic cells in the trephine biopsy specimens. Hypocellular marrow was defined as less than 30% cellularity in patients under the age of 70 years, or less than 20% cellularity in patients 70 years and over.[6] Chromosomal analysis was performed and described according to the International System for Human Cytogenetic Nomenclature (ISCN).[7] Responses to IST were defined according to the established criteria.[8] The ethics committee of Kanazawa University Graduate School of Medical Science approved the study protocol, and all patients provided their informed consent prior to sampling.

Monoclonal antibodies

Monoclonal antibodies (mAbs) used for flow cytometry are shown on the *Online Supplementary Table S1*.

Flow cytometry for detecting GPI-AP$^-$ cells

All blood samples were analyzed within 24 h of collection to avoid false positive results due to cell damage. Staining with each mAb was performed according to the lyse-stain protocol as previously described.[5,9] The presence of CD55 CD59 glycophorin A$^+$ erythrocytes at the level of 0.005% and over and/or CD55 CD59 CD11b$^+$ granulocytes at the level of 0.003% or over was defined as an abnormal increase ('positive') based on the results obtained from 183 healthy individuals.[10] With careful handling of samples and elaborate gating strategies, cut-off values can be lowered to these levels without producing false positive results.[10-12]

Cell sorting and FISH analysis

GPI-AP$^+$ and GPI-AP$^-$ granulocytes from 2 patients with del(13q) (unique patient numbers (UPNs) 3 and 7) were sorted using a FACSAria III cell sorter (BD Bioscience, Franklin Lakes, NJ, USA) and subjected to fluorescence *in situ* hybridization (FISH) analysis using a D13S319-specific probe (Vysis, Voisins-le-Bretonneux, France) as previously described.[13]

Genome analysis of deleted region in patients with del(13q)

Genomic DNA was isolated from peripheral blood cells of 7 patients with del(13q) (UPNs 1, 3, 4, 5, 7, 8 and 22) and subjected to SNP array-based genome-wide analysis of genetic alterations using GeneChip® 250K arrays (Affymetrix, Santa Clara, California, USA) according to the manufacturer's protocol. Genomic and allele-specific copy numbers were calculated using Copy Analyser for GeneChip® (CNAG) software as previously described.[14,15]

Statistical analysis

Prevalence of increased GPI-AP$^-$ cells among different patient populations was compared using the χ^2 test. Time-to-event variables were analyzed using the Kaplan-Meier method, and groups were compared with the log rank test. Two-sided P values were calculated and $P<0.05$ was considered statistically significant. All statistical analyses were performed using the JMP software program version 8.0 (SAS Institute, Cary, NC, USA).

Results and Discussion

Of the 1,228 patients with BM failure, 22 possessed del(13q) (1.8%) that were demonstrated by G-banding; their clinical features are summarized in Table 1. Sixteen patients had only the del(13q) abnormality (which we define as 13q^{-alone}) while the remaining 6 patients had other abnormalities, which we define as 13q^{+other}. Of these 6, 2 had -Y, one had -20, one had del(7q), one had +8, and one had +mar in addition to the del(13q) abnormality. The presence of the del(13q) clone was confirmed by FISH when the number of del(13q) revealed by the G-banding method was less than or equal to two. Median age was 64.5 years old, and BM was hypocellular in 16 patients (12 with 13q^{-alone} and 4 with 13q^{+other}), normocellular in 4 (2 with 13q^{-alone} and 2 with 13q^{+other}), not evaluable in 2 with 13q^{-alone}. All patients with del(13q) were diagnosed with MDS-U due to the absence of significant dysplasia that would fullfill the criteria for MDS as defined by the 2008 WHO classification. All patients were classified as Int-1 according to the International Prognostic Scoring System (IPSS), except for UPN17 who had an IPSS score of 1.5 (Int-2).

As shown in Table 1, GPI-AP$^-$ cells that accounted for from 0.006% to 12.342% (median 0.137%) of granulocytes were detected in all 16 13q^{-alone} patients. FISH analysis of sorted GPI-AP$^-$ and GPI-AP$^+$ granulocytes revealed that del(13q) cells were derived from non-*PIGA* mutant hematopoietic stem cells (HSCs) (Figure 1A). On the other hand, the prevalence of elevated GPI-AP$^-$ cell percentages in 13q^{+other} patients and those with a normal karyotype (637 patients with AA and 300 with MDS) was 50% (3 of 6) and 43% (405 of 937), respectively ($P<0.001$).

Fourteen 13q^{-alone} patients were treated with cyclosporine (CsA) alone,[6] CsA and antithymocyte globulin (ATG)[6] or CsA and anabolic steroids;[2] all achieved either a hematologic improvement in two or three lineages or complete remission (CR), while the response rate to IST in 13q^{+other} patients was 40%. No case was IST-dependent, and response was durable after the cessation of the treatment after patients achieved CR. The clinical course of one patient (UPN 4) who responded to CsA alone and entered CR, despite the fact that G-banding of BM cells showed all 20 dividing cells to be del(13q), has been previously reported.[16] Ninety-six AA patients with the normal karyotype were treated with CsA and ATG (n=47) or CsA±anabolic steroids (n=49). Seventy-eight percent of AA patients responded to IST. Among 19 MDS patients (RCUD, n=14; RCMD, n=5) with a normal karyotype who have been treated with ATG plus CsA (n=3) or CsA with or without anabolic steroids (n=16), 63% responded to IST.

None of the 17 13q^{-alone} patients progressed to advanced MDS or acute myeloid leukemia (AML) during the follow-up period of 3-108 months (median 52 months), while 2 of 6 13q^{+other} patients (one with -20, one with del(7q)) developed AML. The 10-year overall survival rates of patients with 13q^{-alone}, patients with 13q^{+other}, AA patients with a normal karyotype and MDS (RCUD, n=38; RCMD, n=20; MDS-U, n=8) patients with a normal karyotype were 83%, 67%, 85% and 57%, respectively ($P=0.0003$, log rank test on 3 degrees of freedom) (Figure 1B). The 10-year overall survival rates of AA patients with a normal karyotype with and without increased GPI-AP$^-$ cells and MDS (38 with RCUD, 20 with RCMD and 8 with MDS-U) patients with a normal karyotype with and without increased GPI-AP$^-$ cells were 85%, 84%, 66% and 55%, respectively ($P=0.0011$, log rank test on 4 degrees of freedom) (Figure 1C). The percentage of del(13q) clones revealed by G-banding increased in 5 patients and decreased in 3 after successful IST. (*Online Supplementary*

Figure S1) No patient developed clinical features of paroxysmal nocturnal hemoglobinuria (PNH).

SNP array analysis of peripheral blood cells from 7 $13q^{-alone}$ and $13q^{+other}$ patients indicated the region from 13q13.3 to 13q14.3 to be commonly deleted (Figure 1D).

The current retrospective study with a large number of BM failure patients revealed distinctive clinical features of BM failure with del(13q) abnormalities. The 1.8% incidence of del(13q) patients was comparable to that of a recent study (1.9%) based on 2,072 patients with MDS,[17] for which detailed diagnoses of patients with del(13q) were not provided. All del(13q) patients in our study were classified as MDS-U due to the absence of significant dysplasia. We have previously reported that response to IST was remarkably high in 9 patients with del(13q). The present study, which used a different patient cohort, confirmed our previous finding.[2] Between these 22 patients and the 9 patients that we reported in 2002, only 2 developed AML and 22 responded to IST. The overall and leukemia-free survival spans of del(13q) patients treated with IST were as long as AA patients with normal karyotypes treated with IST. These findings suggest that the del(13q) clone in BM failure patients represents the presence of immune pathophysiology rather than clonal disorder associated with AML risk.

Table 1. Clinical features of bone marrow failure patients with del(13q) alone (patients 1-16) or del(13q) plus other abnormalities (patients 17-22).

UPN	Age (years)	Sex	Months from diagnosis to sampling	Dysplasia	Cellularity	Cytogenetics	% of del(13q) cells	Break point	% GPI(-) granulocytes	% GPI(-) RBCs	Previous therapy	Treatment	Response	Outcome	AML transformation	LFS (months)
1	64	F	54	None	hypo	46,XX,del 4/20 (13)(q?)	20	13q(?)	0.042	0.015	No	CsA+AS	HI-2	alive	No	67+
2	42	M	0	None	hypo	46,XY,del(13)(q12q14) 1/20	5	13(q12q14)	3.511	0.562	No	CsA	CR	alive	No	79+
3	47	F	0	None	hypo	46,XX, del(13)(q?) 2/20	10	13q(?)	2.101	0.601	No	ATG+CsA	HI-3	alive	No	24+
4	50	F	4	Erythroid	hypo	46,XX,del(13)(q12q22) 20/20	100	13(q12q22)	0.111	0.013	No	CsA	CR	alive	No	44+
5	65	F	5	None	hypo	46,XX,del(13)(q12q14) 3/20	15	13(q12q14)	0.009	0.008	No	ATG+CsA	CR	alive	No	43+
6	21	M	1	None	hypo	46,XY, del(13)(q?) 6/20	30	13q(?)	0.038	0.003	No	ATG+CsA	HI-3	alive	No	15+
7	52	M	1	Erythroid	NE	46,XY, del(13)(q?) 19/20	95	13q(?)	12.342	0.524	PSL	CsA	HI-3	alive	No	3+
8	87	F	1	None	normo	46,XX,del(13)(q12q22) 9/20	45	13(q12q22)	0.37	0.095	No	CsA	HI-3	alive	No	15+
9	63	F	16	None	hypo	46,XX,del(13)(q12q14) del(13)(q21q31) 5/20	25	13(q12q14), 13(q21q31)	0.006	0.665	PSL	ATG+CsA	HI-3	alive	No	29+
10	74	F	3	None	hypo	46,XX, del(13)(q12q14) 7/13	54	13(q12q14)	0.504	N/A	No	ATG+CsA	HI-3	death (cancer)	No	38
11	54	F	0	None	hypo	46,XX,del(13)(q14q22) 40/40	100	13(q14q22)	0.125	0.008	No	Allo-BMT	NE	alive	No	74+
12	53	M	43	None	hypo	46,XY,del(13)(q14.3)	14	13q14.3	0.281	0.539	No	ATG+CsA	HI-3	alive	No	108+
13	85	M	1	None	hypo	46,XY,del(13)(q?) 2/20	10	13q(?)	0.031	0.01	No	No treatment	NE	death	No	10
14	77	F	3	Erythroid	NE	46,XX,del(13)(q?) 8/20	40	13q(?)	3.125	1.65	No	CsA	CR	alive	No	45+
15	56	M	1	Erythroid	normo	46,XX,del(13)(q12q14) 6/20	30	13(q12q14)	0.069	0.036	No	CsA	HI-2	alive	No	24+
16	74	M	37	None	hypo	46,XY,del(13)(q?) 7/20, 47,X,+Y 7/20	35	13q(?)	0.171	0.441	No	CsA+AS	HI-2	alive	No	52+
17	69	M	1	None	hypo	46,XY,del(7)(q22), del(13)(q12q14) 3/20	15	13(q12q14)	0	0	No	CsA+AS	NR	death	Yes	8
18	68	F	1	None	normo	45,XX,del(13)(q12q22),-20 2/20	10	13(q12q22)	0	0	No	VitK	NE	death	Yes	7
19	75	M	2	None	hypo	45,X,-Y.del(13)(q?) 2/20	10	13q(?)	0	0.003	PSL	CsA	NR	alive	No	71+
20	81	M	17	None	hypo	47,XY,+8,del(13)(q?) 19/20	95	13q(?)	6.851	0.272	No	CsA	NE	alive	No	67+
21	57	F	122	Erythroid	normo	46,XX,del(13),+mar 10/20	50	del(13)	0.522	1.075	AS	CsA+AS	HI-3	alive	No	146+
22	66	M	1	Erythroid	hypo	45,X,-Y,del(13)(q12q14) 15/20	75	13(q12q14)	0.149	0.209	No	CsA	HI-2	alive	No	11+
Median	**65**						**30**		**0.137**	**0.095**						

UPN: unique patient number; M: male; F: female; normo: normocellular marrow; hypo: hypocellular marrow; GPI-AP-granulocytes, glycosylphosphatidyl-inositol anchored protein-deficient granulocytes; GPI-AP-erythrocytes, glycosylphosphatidyl-inositol anchored protein-deficient erythrocytes; CsA: cyclosporine; ATG: antithymocyte globulin; AS: anabolicsteroid; Allo-BMT: allogeneic bone marrow transplant; VitK: vitamin K; CR: complete remission; HI-2: hematologic improvement in two lineages; HI-3: hematologic improvement in three lineages; NR: no response; NE: not evaluable; AML: acute myeloid leukemia; LFS: leukemia-free survival.

Transformation of patient 17 (UPN17) to AML could be attributed to the coexistence of del(7q), which is associated with high risk of AML evolution.[18]

The percentage change of del(13q) clone following IST varied from one patient to another (*Online Supplementary Figure S1*) in a similar way in which the percentage of GPI-AP$^-$ cells changed in the present study (*data not shown*), which is consistent with our previous findings regarding *PIGA* mutant HSCs.[10] Given that effective removal of immune mechanisms by IST does not consistently lower the percentage of del(13q) clone, it is speculated that preferential expansion of del(13q) clones by the immune mechanisms at the onset of BM failure[10] may lead to the escape from immunological pressure, as in the case of *PIGA*

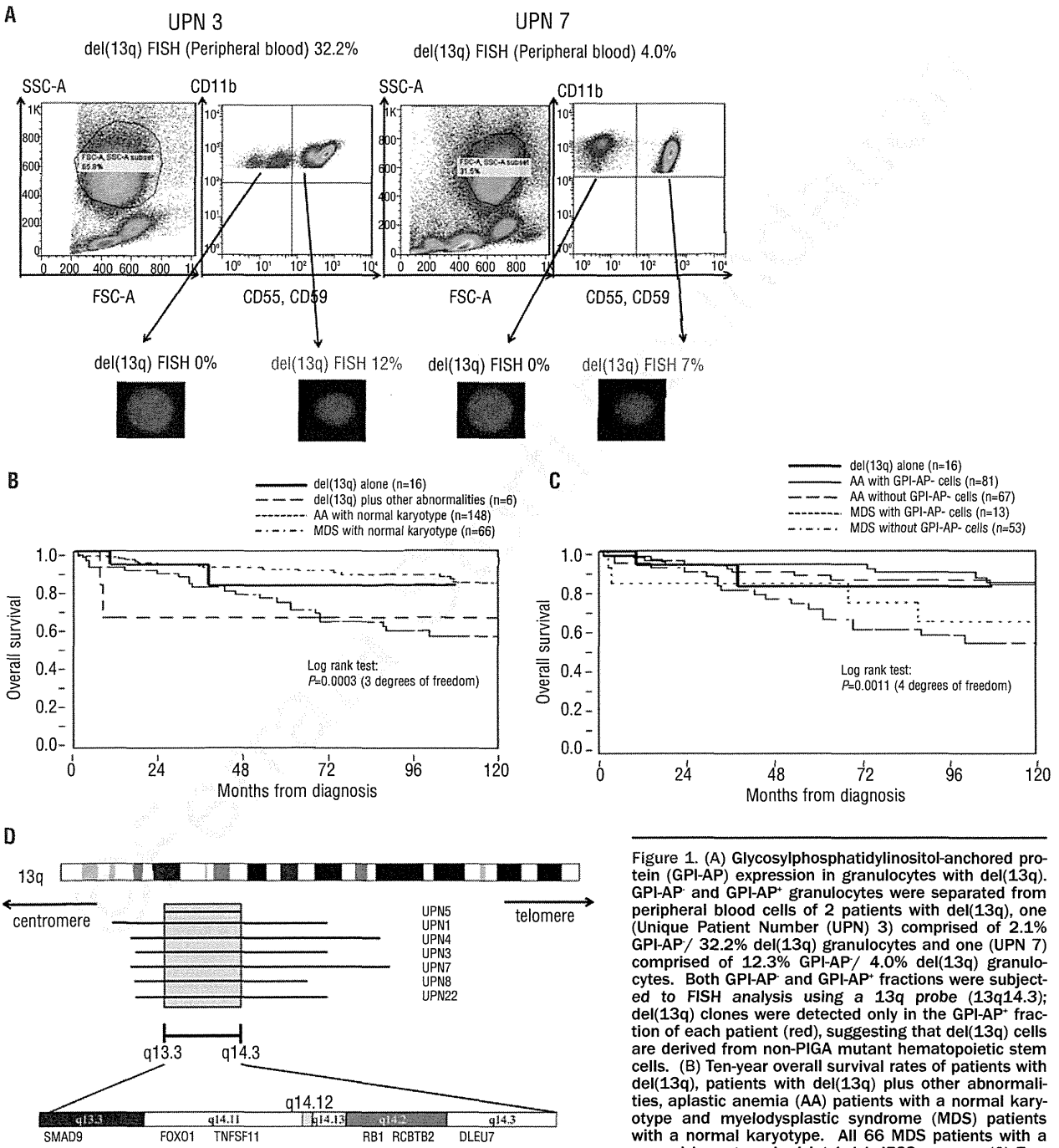

Figure 1. (A) **Glycosylphosphatidylinositol-anchored protein (GPI-AP) expression in granulocytes with del(13q). GPI-AP$^-$ and GPI-AP$^+$ granulocytes were separated from peripheral blood cells of 2 patients with del(13q), one (Unique Patient Number (UPN) 3) comprised of 2.1% GPI-AP$^-$/ 32.2% del(13q) granulocytes and one (UPN 7) comprised of 12.3% GPI-AP$^-$/ 4.0% del(13q) granulocytes. Both GPI-AP$^-$ and GPI-AP$^+$ fractions were subjected to FISH analysis using a 13q probe (13q14.3); del(13q) clones were detected only in the GPI-AP$^+$ fraction of each patient (red), suggesting that del(13q) cells are derived from non-PIGA mutant hematopoietic stem cells.** (B) **Ten-year overall survival rates of patients with del(13q), patients with del(13q) plus other abnormalities, aplastic anemia (AA) patients with a normal karyotype and myelodysplastic syndrome (MDS) patients with a normal karyotype. All 66 MDS patients with a normal karyotype had Int-1-risk IPSS scores.** (C) **Ten-year overall survival rates of patients with del(13q), aplastic anemia (AA) patients with a normal karyotype with and without increased GPI-AP$^-$ cells and myelodysplastic syndrome (MDS) patients with a normal karyotype with and without increased GPI-AP$^-$ cells.** (D) **Deleted gene loci regions of 7 patients with del(13q), shown as bold horizontal lines for each UPN under the gene. The shaded box represents the deleted region common to patients, 13q13.3 to 13q14.3, which encodes proteins involved in cytokine signal transduction.**

mutant HSCs. It is necessary to identify common mechanisms leading to preferential activation of both PIGA mutant HSCs and HSCs with del(13q) in immune-mediated BM failure to verify these hypotheses.

A possible immune pathophysiology in $13q^{-alone}$ patients is supported by the markedly high prevalence (100%) of elevated GPI-AP$^-$ cell levels which is linked to the escape of *PIGA* mutant HSCs from an immune system attack.[19] Because the del(13q) abnormality occurs in the GPI-AP$^+$ population, it may play a similar role to the GPI-AP$^-$ cells. SNP array analysis revealed the common deletion of a 15 Mb (13.3 to 14.3) region of 13q in 7 $13q^{-alone}$ and $13q^{-+other}$ patients. This segment encodes several proteins that regulate cell proliferation and the cell cycle, such as SMAD9 and RB1; both are involved in the signal transduction pathway of transforming growth factor-beta (TGF-β, an important cytokine in regulating HSC dormancy. Cytokine-mediated selection of *PIGA* mutant HSCs has been proposed as a mechanism for preferential proliferation of GPI-AP$^-$ cells,[20] but no supporting evidence has been presented. A previous study demonstrated that GPI-AP$^-$ T cells show decreased sensitivity to herpes virus entry mediator (HVEM) ligands that transmit inhibitory signals through receptors for CD160(21) and TGF-β.[22,23] The presence of del(13q) represents a unique subgroup of immune-mediated BM failure associated with an increase in the percentage of GPI-AP$^-$ cells, where del(13q) and *PIGA* mutant HSCs undergo preferential expansion, possibly due to their decreased sensitivity to cell-cycle inhibitory molecules, such as TGF-β compared to normal HSCs.

In conclusion, MDS-U with del(13q) alone is a benign BM failure syndrome characterized by a good response to IST and a markedly high prevalence of elevated GPI-AP$^-$ cell percentages. Therefore, del(13q) should be eliminated from the list of karyotypic abnormalities representing the intermediate group defined by IPSS,[24] and BM failure with del(13q) should be managed as AA.

Authorship and Disclosures

The information provided by the authors about contributions from persons listed as authors and in acknowledgments is available with the full text of this paper at www.haematologica.org.

Financial and other disclosures provided by the authors using the ICMJE (www.icmje.org) Uniform Format for Disclosure of Competing Interests are also available at www.haematologica.org.

References

1. Schanz J, Steidl C, Fonatsch C, Pfeilstocker M, Nosslinger T, Tuechler H, et al. Coalesced multicentric analysis of 2,351 patients with myelodysplastic syndromes indicates an underestimation of poor-risk cytogenetics of myelodysplastic syndromes in the international prognostic scoring system. J Clin Oncol. 2011;29(15):1963-70.
2. Ishiyama K, Karasawa M, Miyawaki S, Ueda Y, Noda M, Wakita A, et al. Aplastic anaemia with 13q-: a benign subset of bone marrow failure responsive to immunosuppressive therapy. Br J Haematol. 2002;117 (3):747-50.
3. Sloand EM, Olnes MJ, Shenoy A, Weinstein B, Boss C, Loeliger K, et al. Alemtuzumab treatment of intermediate-1 myelodysplasia patients is associated with sustained improvement in blood counts and cytogenetic remissions. J Clin Oncol. 2010;28(35): 5166-73.
4. Wang H, Chuhjo T, Yasue S, Omine M, Nakao S. Clinical significance of a minor population of paroxysmal nocturnal hemoglobinuria-type cells in bone marrow failure syndrome. Blood. 2002;100(12):3897-902.
5. Sugimori C, Chuhjo T, Feng X, Yamazaki H, Takami A, Teramura M, et al. Minor population of CD55-CD59- blood cells predicts response to immunosuppressive therapy and prognosis in patients with aplastic anemia. Blood. 2006;107(4):1308-14.
6. Yue G, Hao S, Fadare O, Baker S, Pozdnyakova O, Galili N, et al. Hypocellularity in myelodysplastic syndrome is an independent factor which predicts a favorable outcome. Leuk Res. 2008; 32(4):553-8.
7. International Standing Committee on Human Cytogenetic Nomenclature. Shaffer LG, Slovak ML, Campbell LJ. ISCN 2009: an international system for human cytogenetic nomenclature (2009). Basel; Unionville, CT: Karger; 2009. vi, 138.
8. Cheson BD, Greenberg PL, Bennett JM, Lowenberg B, Wijermans PW, Nimer SD, et al. Clinical application and proposal for modification of the International Working Group (IWG) response criteria in myelodysplasia. Blood. 2006;108(2):419-25.
9. Araten DJ, Nafa K, Pakdeesuwan K, Luzzatto L. Clonal populations of hematopoietic cells with paroxysmal nocturnal hemoglobinuria genotype and phenotype are present in normal individuals. Proc Natl Acad Sci USA. 1999;96(9):5209-14.
10. Sugimori C, Mochizuki K, Qi Z, Sugimori N, Ishiyama K, Kondo Y, et al. Origin and fate of blood cells deficient in glycosylphosphatidylinositol-anchored protein among patients with bone marrow failure. Br J Haematol. 2009;147(1):102-12.
11. Kulagin A, Golubovskaya I, Ganapiev A, Babenko E, Sipol A, Pronkina N, et al. Prognostic value of minor PNH clones in aplastic anaemia patients treated with ATG-based immunosuppression: results of a two-centre prospective study. Bone Marrow Transplant. 2011;46:S83-S4.
12. Parker C, Omine M, Richards S, Nishimura J, Bessler M, Ware R, et al. Diagnosis and management of paroxysmal nocturnal hemoglobinuria. Blood. 2005;106(12):3699-709.
13. Facon T, Avet-Loiseau H, Guillerm G, Moreau P, Genevieve F, Zandecki M, et al. Chromosome 13 abnormalities identified by FISH analysis and serum beta2-microglobulin produce a powerful myeloma staging system for patients receiving high-dose therapy. Blood. 2001;97(6):1566-71.
14. Nannya Y, Sanada M, Nakazaki K, Hosoya N, Wang L, Hangaishi A, et al. A robust algorithm for copy number detection using high-density oligonucleotide single nucleotide polymorphism genotyping arrays. Cancer Res. 2005;65(14):6071-9.
15. Yamamoto G, Nannya Y, Kato M, Sanada M, Levine RL, Kawamata N, et al. Highly sensitive method for genomewide detection of allelic composition in nonpaired, primary tumor specimens by use of affymetrix single-nucleotide-polymorphism genotyping microarrays. Am J Hum Genet. 2007;81(1): 114-26.
16. Kasahara I, Nishio M, Endo T, Fujimoto K, Koike T, Sugimori N, et al. Sustained trilineage hematopoietic recovery in a patient with refractory anemia, del(13)(q12q22), and paroxysmal nocturnal hemoglobinuria-type cells treated with immunosuppressive therapy. Leuk Res. 2011;35(9):e147-8.
17. Haase D. Cytogenetic features in myelodysplastic syndromes. Ann Hematol. 2008;87 (7):515-26.
18. Maciejewski JP, Risitano A, Sloand EM, Nunez O, Young NS. Distinct clinical outcomes for cytogenetic abnormalities evolving from aplastic anemia. Blood. 2002;99(9): 3129-35.
19. Rotoli B, Luzzatto L. Paroxysmal nocturnal haemoglobinuria. Baillieres Clin Haematol. 1989;2(1):113-38.
20. Parker CJ. The pathophysiology of paroxysmal nocturnal hemoglobinuria. Exp Hematol. 2007;35(4):523-33.
21. Cai G, Anumanthan A, Brown JA, Greenfield EA, Zhu B, Freeman GJ. CD160 inhibits activation of human CD4+ T cells through interaction with herpesvirus entry mediator. Nat Immunol. 2008;9(2):176-85.
22. Yamazaki S, Iwama A, Takayanagi S, Eto K, Ema H, Nakauchi H. TGF-beta as a candidate bone marrow niche signal to induce hematopoietic stem cell hibernation. Blood. 2009;113(6):1250-6.
23. Katagiri T, Qi Z, Ohtake S, Nakao S. GPI-anchored protein-deficient T cells in patients with aplastic anemia and low-risk myelodysplastic syndrome: implications for the immunopathophysiology of bone marrow failure. Eur J Haematol. 2011;86(3):226-36.
24. Greenberg P, Cox C, LeBeau MM, Fenaux P, Morel P, Sanz G, et al. International scoring system for evaluating prognosis in myelodysplastic syndromes. Blood. 1997;89 (6):2079-88.

STEM CELLS®

TISSUE-SPECIFIC STEM CELLS

Individual Hematopoietic Stem Cells in Human Bone Marrow of Patients with Aplastic Anemia or Myelodysplastic Syndrome Stably Give Rise to Limited Cell Lineages

TAKAMASA KATAGIRI,[a,b] HIROSHI KAWAMOTO,[c] TAKASHI NAKAKUKI,[d] KEN ISHIYAMA,[b] MARIKO OKADA-HATAKEYAMA,[e] SHIGEKI OHTAKE,[a] YU SEIKI,[b] KOHEI HOSOKAWA,[b] SHINJI NAKAO[b]

[a]Clinical Laboratory Science, Division of Health Sciences, and Kanazawa University Graduate School of Medical Science, Kanazawa, Ishikawa, Japan; [b]Cellular Transplantation Biology, Kanazawa University Graduate School of Medical Science, Kanazawa, Ishikawa, Japan; [c]Laboratory for Lymphocyte Development and [e]Laboratory for Cellular Systems Modeling, RIKEN Research Center for Allergy and Immunology, Tsurumi-ku, Yokohama, Kanagawa, Japan RIKEN Research Center for Allergy and Immunology, Tsurumi-ku, Yokohama, Kanagawa, Japan; [d]Department of Mechanical Systems Engineering Faculty of Engineering, Kogakuin University, Shinjuku-ku, Tokyo, Japan.

Key Words. Differentiation • Experimental models • Fluorescence-activated cell sorting • Hemopoietic stem cells • Hematopoietic progenitors • Aplastic anemia • Bone marrow

ABSTRACT

Mutation of the phosphatidylinositol *N*-acetylglucosaminyltransferase subunit A (*PIG-A*) gene in hematopoietic stem cells (HSCs) results in the loss of glycosylphosphatidylinositol-anchored proteins (GPI-APs) on HSCs, but minimally affects their development, and thus can be used as a clonal maker of HSCs. We analyzed GPI-APs expression on six major lineage cells in a total of 574 patients with bone marrow (BM) failure in which microenvironment itself is thought to be unaffected, including aplastic anemia (AA) or myelodysplastic syndrome (MDS). GPI-APs-deficient (GPI-APs$^-$) cells were detected in 250 patients. Whereas the GPI-APs$^-$ cells were seen in all six lineages in a majority of patients who had higher proportion ([dbmtequ]3%) of GPI-APs$^-$ cells, they were detected in only limited lineages in 92.9% of cases in the lower proportion (<3%) group. In all 250 cases, the same lineages of GPI-APs$^-$ cells were detected even after 6–18-month intervals, indicating that the GPI-APs$^-$ cells reflect hematopoiesis maintained by a self-renewing HSC in most of cases. The frequency of clones with limited lineages seen in mild cases of AA was similar to that in severe cases, and clones with limited lineages were seen even in two health volunteer cases. These results strongly suggest most individual HSCs produce only restricted lineages even in a steady state. While this restriction could reflect heterogeneity in the developmental potential of HSCs, we propose an alternative model in which the BM microenvironment is mosaic in supporting commitment of progenitors toward distinct lineages. Our computer simulation based on this model successfully recapitulated the observed clinical data. STEM CELLS *2013;31:536–546*

Disclosure of potential conflicts of interest is found at the end of this article.

INTRODUCTION

To sustain hematopoiesis, hematopoietic stem cells (HSCs) must, on the one hand, replenish themselves by self-renewal and on the other hand produce differentiating progenitor cells. It is also known that most HSCs remain dormant and are only rarely and randomly activated. It has been estimated that each human possesses a total of 10^4 HSCs, and that ~400 HSCs actively contribute to hematopoiesis, replicating once per year [1, 2]. However, the actual dynamics of hematopoiesis by HSCs remains uncertain. For example, it is unclear how long an individual HSC maintains hematopoiesis and whether all major lineage cells are produced from a single HSC. These issues have been difficult to address due to the lack of appropriate experimental systems, regardless of animal species.

In the case of humans, however, we were led to consider one "experiment of nature" that makes it possible to track the

Author contributions: H.K.: developed the concept of the study and supervised the project, designed the experiments, wrote the paper, and approved the final version of this paper; S.N.: developed the concept of the study and supervised the project, wrote the paper, and approved the final version of this paper; T.K. and T.N.: designed the experiments, performed the experiments and analyzed the data, wrote the paper, and approved the final version of this paper; K.I. and M.O.-H.: designed the experiments and approved the final version of this paper; S.O., Y.S. and K.H. :performed the experiments and analyzed the data, approved the final version of this paper. T.K., H.K., and T.N. contributed equally to this article.

Correspondence: Shinji Nakao, M.D., Ph.D., Cellular Transplantation Biology, Kanazawa University Graduate School of Medical Science, 13-1 Takara-machi, Kanazawa, Ishikawa 920-8640, Japan. Telephone: +81-76-265-2274; Fax: +81-76-234-4252; e-mail: snakao8205@staff.kanazawa-u.ac.jp Received September 21, 2012; Revised November 12, 2012; accepted for publication November 26, 2012; first published online in STEM CELLS *EXPRESS* January 12, 2013. 1066-5099/2013/$30.00/0 doi: 10.1002/stem.1301

progeny of a HSC; that is, by detecting blood cells deficient in glycosylphosphatidylinositol-anchored proteins (GPI-APs) using flow cytometry. GPI-APs-deficient (GPI-APs$^-$) blood cells are rarely detectable in healthy individuals, but are a common feature in paroxysmal nocturnal hemoglobinuria (PNH) and are also frequently seen in patients with bone marrow (BM) failure such as aplastic anemia (AA) or myelodysplastic syndrome (MDS). These cells are known to be derived from HSCs with a mutation in the phosphatidylinositol *N*-acetylglucosaminyltransferase subunit A (*PIG-A*) gene. MDS cases harboring GPI-APs$^-$ blood cells are characterized by polyclonal hematopoiesis and good response to immunosuppressive therapy, and are therefore thought to be similar to AA in their pathophysiology [3].

The *PIG-A* mutant HSCs used to be thought to have greater proliferative capacity than normal HSCs because one or a few *PIG-A* mutant clones sometimes account for a large proportion of hematopoietic cells for long period in PNH patients [4]. However, several reports instead indicate that the mutant HSCs in most PNH patients have properties similar to normal HSCs: for example, no growth advantage over wild-type HSCs [5, 6], genetic stability and extremely low incidence of secondary mutations [2, 7–9], and the rarity of leukemic cell evolution of GPI-APs$^-$ cells in PNH patients [10].

We recently found that GPI-APs$^-$ cells in patients with AA and MDS frequently show various patterns in the proportion of granulocytes and erythrocytes and that the individual patterns of the two lineage combinations can persist for many years. The percentage of GPI-APs$^-$ cells in some patients remained almost the same over 10 years even when the percentages were less than 1% [11]. In such stable cases, it is quite likely that GPI-APs$^-$ peripheral blood (PB) cells are produced from HSC(s), and that the GPI-APs$^-$ HSC itself as well as its surrounding environment is largely normal, at least during the observation period. Indeed, BM environment itself in the patients to support hematopoiesis is thought to be largely normal, since these cases are thought to be caused by immune reaction against blood cells. It is also highly probable that the whole GPI-APs$^-$ cells in each patient represent a clone, originating from a single HSC in which *PIG-A* mutation occurred, since it is statistically rare that the *PIG-A* mutation occurs twice in one patient. Although it is unclear that such a clone is maintained by a single HSC or multiple descendent HSCs, it can be said that the kinetics of GPI-APs$^-$ cells during stable period reflect the regular hematopoietic events originally initiated by a single HSC. We then thought that it could be very much informative if we extend our analysis to cover various hematopoietic lineages in addition to erythrocytes and granulocytes. We therefore determined the proportion of GPI-APs$^-$ cells in six major lineages, namely granulocytes (G), monocytes (M), erythrocytes (E), T cells (T), Natural Killer cells (NK), and B cells (B), in PB cells from BM failure patients using a highly sensitivity flow cytometric analysis [12].

Materials and Methods

Patients and Healthy Volunteers

The PB of 574 patients with various types of cytopenias was examined for the presence of GPI-APs$^-$ cells using high sensitivity flow cytometry. Their diagnoses included AA in 354 (39 with very severe, 92 with severe, and 223 with nonsevere AA [13]), MDS-refractory anemia (RA) defined by the french-american-british (FAB) classification [14] in 207, and classic PNH in 13. The male to female ratio was 1:1.2 (261:313) and the median age was 57 years (range: 1–95 years). PB samples from 192 healthy individuals were also examined for the presence of GPI-APs$^-$ cells in all lineages of cells. All patients and healthy individuals including next of kin on the behalf of minors/children participants in our study provided their informed written consent before sampling. This study protocol was approved by the ethics committee of Kanazawa University Graduate School of Medical Science.

Monoclonal Antibodies

Monoclonal antibodies (mAbs) used for multicolor flow cytometry were anti-CD59 labeled with FITC (P282E, IgG2a; Beckman Coulter, Miami, FL, http://www.labome.com/product/Beckman-Coulter-Inc/IM3457U.html), anti-CD55 labeled with FITC (IA10, IgG2a; BD Pharmingen,http://www.bdbiosciences.com/external_files/pm/doc/tds/human/live/web_enabled/33574X_555693.pdf), anti-CD48 labeled with FITC (J4-57, IgG1; Beckman Coulter, http://www.bionity.com/en/antibodies/beckman-IM1837U/cd48-anti-human-klon-j4-57.html), anti-CD33 labeled with APC (D3HL60.251, IgG1; Beckman Coulter, http://www.bionity.com/en/antibodies/beckman-A70200/cd33-anti-human-klon-d3hl60-251.html), anti-CD19 labeled with APC-Cy7 (SJ25C1, IgG1; BD Pharmingen, http://www.bdbiosciences.com/external_files/pm/doc/tds/human/live/web_enabled/557791.pdf), anti-CD335 labeled with Phycoerythrin (BAB281, IgG1; Beckman Coulter, http://www.bc-cytometry. com/DataSheetPDF/IM3711_D.S.pdf), anti-CD3 labeled with PerCPCy5.5 (SK7, IgG1; BD Pharmingen, http://www.bdbiosciences.com/documents/BD_PerCP-Cy5.5_and_PerCP.pdf), anti-CD11b/Mac-1 labeled with PE (ICRF44, IgG1; BD Pharmingen, http://www4.bdj.co.jp/ecat/txDetailedTable.jsp?size=20&item=746256&form=formNavigator&action=LIST_PAGE&pageItem=45), and anti-glycophorin A labeled with PE (JC159, IgG1; Dako, Carpenteria, CA, http://www.dako.com/us/index/flow_cytometry_catalog_us.pdf).

Flow Cytometry for Detecting GPI-APs$^-$ Cells

Six lineages of blood cells including granulocytes, erythrocytes, monocytes, T cells, B cells, and NK cells were subjected to high sensitivity flow cytometry for detecting small populations of GPI-APs$^-$ cells. All blood samples were analyzed within 24 hours to avoid false-positive results due to cell damage. The staining with the each mAb in this study was performed according to the well-established lyse-stain protocol, previously described in detail [12, 15]. Briefly, 3–5 mL of heparinized blood was drawn from the patients and healthy individuals. Erythrocytes were lysed in a lysis buffer (Roche Applied Science, Nagoya, Japan, http://roche-biochem.jp/catalog/index.php/product_3.6.6.4.42.1.html) containing NH_4Cl 8.26 g/L, $KHCO_3$ 1.0 g/L, and EDTA·E_4Na 0.037 g/L to detect GPI-APs$^-$ leukocytes. After washing with saline, 50 μL of the leukocyte suspension was incubated with FITC-labeled anti-CD55 and anti-CD59 mAbs for granulocytes or FITC-labeled anti-CD48 and anti-CD59 mAbs for monocytes, T cells, B cells, and NK cells in combination with mAbs specific for lineage markers including PE-labeled CD11b for granulocytes, APC-labeled CD33 for monocytes, PerCP-Cy5.5-labeled CD3 for T cells, APC-Cy7-labeled CD19 for B cells, and PE-labeled CD335 for NK cells. Fresh blood was diluted to 3% in phosphate-buffered saline (PBS), and then 50 μL was incubated with PE-labeled anti-glycophorin A and FITC-labeled anti-CD55 and anti-CD59 mAbs on ice for 30 minutes to detect GPI-APs$^-$ erythrocytes. Three-step gating excluded debris and immature granulocytes that are frequently found in samples from patients with MDS. Step 1 involved the gating of granulocyte, lymphocyte, or monocyte populations from the Forward Scatter (FSC)-Side Scatter (SSC) scattergrams (R1). Step 2 involved the gating of the lineage marker^{bright} population on the lineage marker-SSC scattergram to exclude the lineage marker^{dim} cells that are features of either damaged cells or immature cells. Step 3 was the gating of R1 × R2 and the analysis of 10^6 cells on R1 × R2 scattergrams. The following cut-off values that had been determined by our

previous studies based on 183 healthy individuals were used; the presence of ≥0.005% $CD55^-CD59^-$ glycophorin A^+ erythrocytes, ≥0.003% $CD55^-CD59^-CD11b^+$ granulocytes, and ≥0.01% $CD48^-CD59^-CD33^+$ monocytes, $CD48^-CD59^-CD3^+$ T cells, $CD48^-CD59^-CD19^+$ B cells, and $CD48^-CD59^-CD335^+$ NK cells [12, 16]. When GPI-APs$^-$ cells were detected in only one lineage of cells or the percentages of GPI-APs$^-$ cells were less than 0.01%, then additional samples were tested, and the patients were judged to be positive for increased GPI-APs$^-$ (PNH^+) when the analysis results of the first and second samples were identical. Data acquisition was performed immediately after the sample preparation using a FACSCanto II instrument (Beckton Dickinson) and the data were analyzed using the FACSDiva software program and the percentage of each population was calculated by FlowJo software 7.6.1 (Tree star, Inc., Ashland, OR).

Cell Sorting and *PIG-A* Gene Analysis

Freshly isolated GPI-APs$^-$ cells were separated from GPI-APs$^+$ fraction using a FACSAria II instrument (Beckton Dickinson). More than 95% of the sorted cells were GPI-APs deficient. An analysis of the *PIG-A* gene mutation was performed as described previously [17]. Briefly, the coding regions of *PIG-A* were amplified by nested or seminested PCR using 12 primer sets, and six ligation reactions were used to transform competent *Escherichia coli* JM109 cells (Nippon Gene, Japan, http://www.nippongene.com/pages/products/genetransfer/ecos/index.html). Five clones were selected randomly from each group of transfectants and subjected to sequencing with BigDye Terminator v3.1 Cycle Sequencing kit (Applied Biosystems, San Diego, CA,http://www3.appliedbiosystems.com/cms/groups/mcb_support/documents/generaldocuments/cms_042772.pdf) and an ABI PRISM 3100 Genetic Analyzer (Applied Biosystems).

Simulation of the Blood Cell Production by HSCs

Migration, division, lineage determination, and death of clones of a HSC in BM environment are simulated with a lattice Monte Carlo method. For efficient simulation, we focused on the events on a cross-section of BM, which enabled us to perform two-dimensional simulation. The occurrence of events was managed with their transition probabilities and the simulation was executed on the basis of actual time. We used the hybrid null-event Monte Carlo algorithm [18, 19], and here outline the model description and simulation setup (also see Supporting Information Note for detailed information). A square area (30 mm × 30 mm) that is large enough to encompass some commitment planes is represented using 1,500 × 1,500 square lattices (20 μm × 20 μm each). Initially, a HSC is randomly added to a site, and then it continues to create clones once per 10 hours until there have been five divisions. Clones randomly move along the lattice with the transition probability and undergo cell division once per 8–12 hours. We assume that lineage determination occurs after the fifth division, based on the site of the clone in the mosaic-like hematopoietic environment where each site supports differentiation into M, E, B, or T-cell lineages. In addition, the lineage clone becomes a mature cell after a further five divisions under the condition that it can divide only in the sites that support differentiation into the same lineage. Otherwise, cell death results after 48-hour movement on areas that support other lineages, although all clones die 72 hours after maturation.

We also investigated the relation between clone size and the number of emerging cell lineages. In our simulation, clone size is dominated by the setting of "N times divisions for lineage determination and further N times divisions for maturing." We simply change the number N in a range of 3–12. For each N, 128 simulations starting from randomly selected initial sites of HSCs are executed for 120 simulation hours. For each simulation, the number of cell lineages is counted, and clone size is calculated as the maximum number of clones for the entire simulation period.

Results

GPI-APs$^-$ Cells Were Seen in Various Combination of Lineages of Blood Cells from BM Failure Patients

Of 574 patients with BM failure, GPI-APs$^-$ cells were detected in at least one lineage of cells of 250 patients (44%). The prevalences of increased GPI-APs$^-$ cells were 56% in AA and 19% in MDS-RA. The proportion of GPI-APs$^-$ cells among granulocytes ranged 0.003%–99.1%, with mean and median value 5.38% and 0.19%, respectively. GPI-APs$^-$ cells were rather frequently found in patients with less severe AA; the prevalences were 63% in nonsevere, 49% in severe, and 31% in very severe AA patients. The lineage combinations of GPI-APs$^-$ cells in patients possessing GPI-APs$^-$ cells (PNH^+ patients) were classified into 16 different patterns (Supporting Information Table S1). Figure 1 shows representative flow cytometric profiles of one healthy individual and four patients showing Granulocyte, Monocyte, Erythrocyte, T cell, NK cell, B cell (GMETNKB), Granulocyte, Monocyte, Erythrocyte (GME), Granulocyte, Monocyte, Erythrocyte, T cell, NK (GMETNK), or Granulocyte, Monocyte, Erythrocyte, B cell (GMEB) patterns.

Clone Size of GPI-APs$^-$ Granulocytes Correlates with the Number of Cell Lineages that Contain GPI-APs$^-$ Cells

The percentages of GPI-APs$^-$ granulocytes in each group bearing GPI-APs$^-$ cells in one to six lineages are plotted in Figure 2. There was a clear trend toward the pattern of the higher the percentage of GPI-APs$^-$ granulocytes in patients, the greater the number of GPI-APs$^-$ cell lineages.

In order to closely examine the relationship between the severity of AA and the GPI-APs$^-$ clone size, we arbitrarily classified AA patients in this study into five categories, namely stages 1, 2, and 3 (nonsevere), stage 4 (severe), and stage 5 (very severe), based on the severity of cytopenias (Supporting Information Table S2) and replotted the data (Fig. 2B). Patients with higher proportion (>1%) of GPI-APs$^-$ granulocytes were not seen in nonsevere cases, suggesting that the clone size of GPI-APs$^-$ cells correlates with severity of BM failure. The notable observation here is that the correlation between the percentage of GPI-APs$^-$ granulocytes and the number of GPI-APs$^-$ cell lineages is almost identical in all three groups. This finding may indicate that the production of limited lineage cells observed in smaller clones is not due to the possible functional failures of BM microenvironment. It seems more likely that "fewer lineages in smaller clones" instead represents events occurring in normal hematopoiesis.

Persistence of GPI-APs$^-$ Lineage Combination Over a Long Period

We then reexamined PB cells of 250 patients 6–18 months after the first examination and to our surprise, GPI-APs$^-$ cells were observed in all 250 patients. Detection of GPI-APs$^-$ cells after such a long interval indicates that the GPI-APs$^-$ cells are most likely derived from HSCs rather than from non-self-renewing progenitors. Of special interest was our finding that in all 250 cases, the same combinations of lineages were detected regardless of the interval between the first and second analysis. Flow cytometric profiles of various lineages of a case representing Granulocyte, Monocyte, Erythrocyte, T cell (GMET) type are shown in Figure 3. Figure 4 shows the proportion of GPI-APs$^-$ cells in each lineage in the first and second analysis for a total of representative 25 cases (five cases for each type).

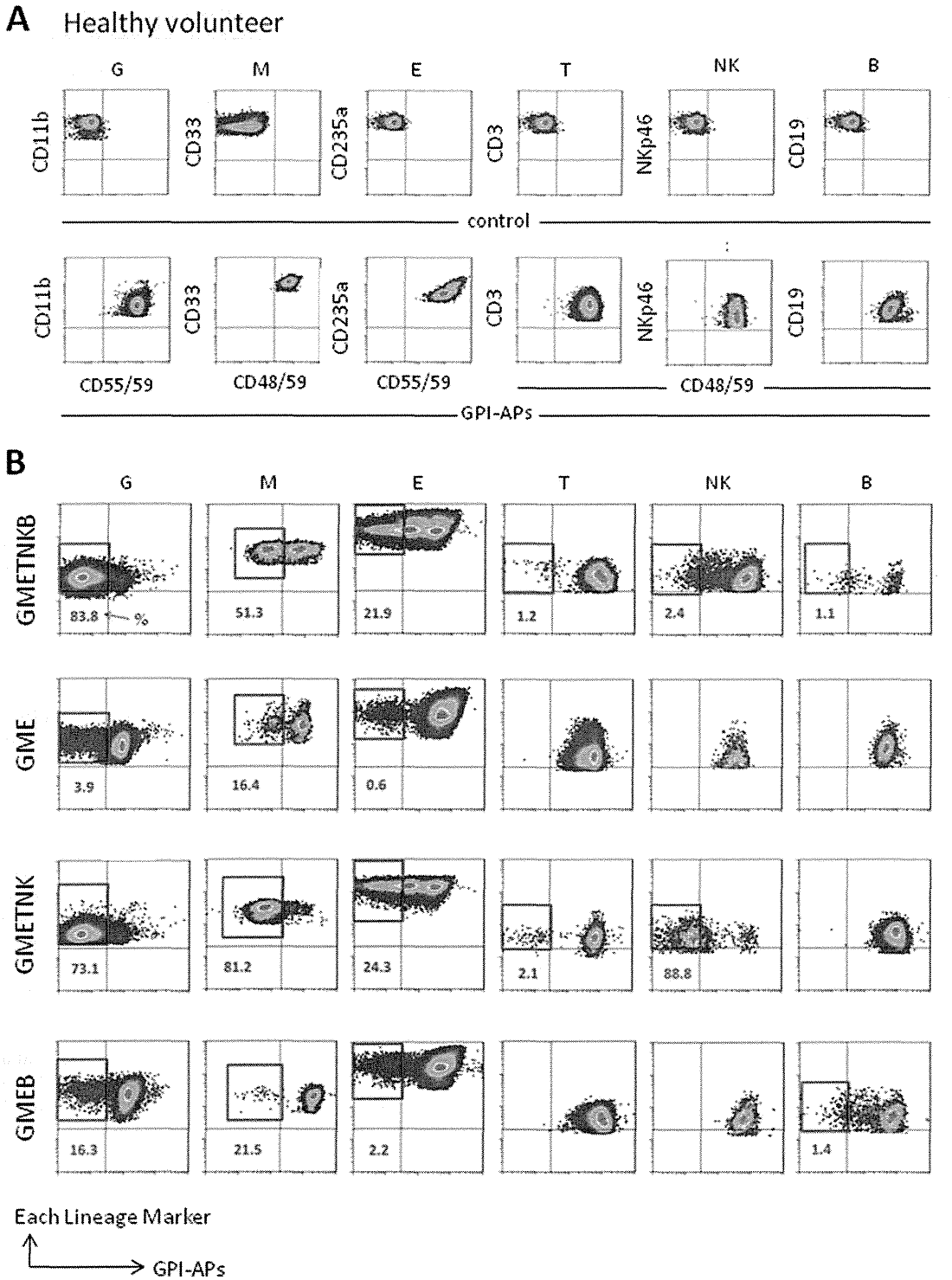

Figure 1. Detection of GPI-APs$^-$ cells in different lineages of blood cells. **(A):** One example of peripheral blood (PB) cells of a healthy individual having no GPI-APs$^-$ cells. **(B):** GPI-APs$^-$ cell combination patterns in four patients. Profiles of PB cells of patients showing GPI-APs$^-$ cells in GMETNKB, GME, GMETNK, and GMEB lineages are shown. Lineage markers used were CD11b for G, CD33 for M, glycophorin-A (CD235a) for E, CD3 for T, NKp46 for NK, and CD19 for B. G, M, E, T, NK, or B stands for granulocytes, monocytes, erythrocytes, T cells, NK cells, or B cells, respectively. Abbreviations: GPI-APs, glycosylphosphatidylinositol-anchored proteins; GME, Granulocyte, Monocyte, Erythrocyte.

PIG-A Gene Mutations in Different Lineages of Blood Cells

To confirm their clonal origin, GPI-APs$^-$ cells sorted from five patients were subjected to *PIG-A* gene analysis. The same mutation was identified in different lineages in three patients (Supporting Information Table S3). In GPI-APs$^-$ granulocytes with other lineages from Patients 16, 1, and 5 and GPI-APs$^-$ granulocytes from Patients 9 and 30, the same

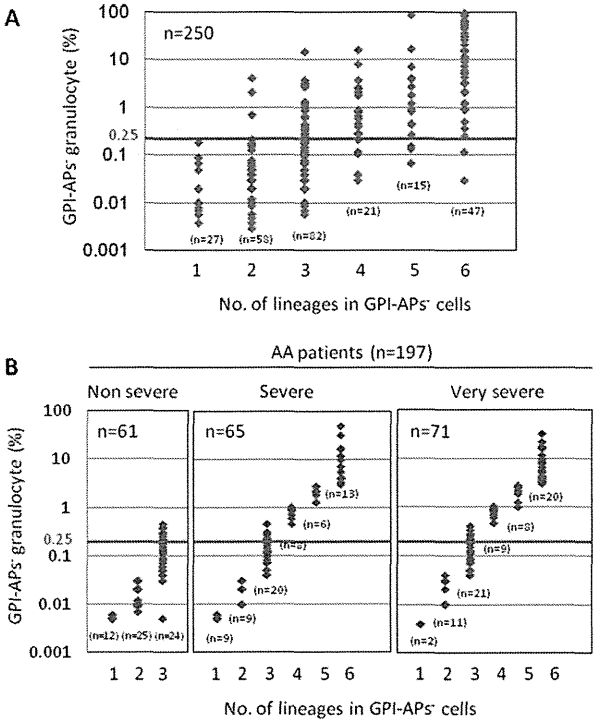

Figure 2. Correlation between the clone size of GPI-APs$^-$ granulocytes and the number of cell lineages that contain GPI-APs$^-$ cells. **(A):** The percentage of GPI-APs$^-$ granulocytes and the number of cell lineages that contain GPI-APs$^-$ cells in individual patients are plotted. A red line for 0.25% stands for the expected value for an average size of a single hematopoietic stem cell clone. **(B):** The percentage of GPI-APs$^-$ granulocytes and the number of cell lineages that contain GPI-APs$^-$ cells in AA patients, classified in three categories according to the severity of disease (stage 1 or 2, stage 3, and stage 4 or 5), are plotted. AA patients were classified into five categories based on the disease severity (stage 1 or 2, stage 3, and stage 4 or 5) (Supporting Information Table S2). Abbreviation: GPI-APs, glycosylphosphatidylinositol-anchored proteins.

mutation was found 3–7 months after the initial analyses. Therefore, it is highly probable that in most, if not all, cases the GPI-APs$^-$ cells are clonal [20]. This finding is in line with the estimation that PNH patients only rarely have more than two clones at the HSC level [8, 9].

GPI-APs$^-$ Cells Were Detected in Limited Lineages in Healthy Volunteers Over a Long Period

Dormant HSCs with *PIG-A* mutation reside in the BM and can be activated albeit uncommonly [17]. If this hypothesis is tenable, small populations of GPI-APs$^-$ cells may be detectable in some healthy individuals. We then examined PB of 192 healthy volunteers for the presence of GPI-APs$^-$ cells. Notably, two were found to bear detectable levels of GPI-APs$^-$ cells, and in both of them GPI-APs$^-$ cells were detected in limited lineages, representing GME and GE type (Fig. 5A). The two healthy cases bearing GPI-APs$^-$ cells were situated within the range of distribution of AA and MDS cases in terms of chimerism ratio versus lineage number (Fig. 5B), further supporting that findings seen in AA and MDS cases reflect normal hematopoiesis.

As described in Introduction, the number of active human HSCs at any given time is estimated to be around 400. It is therefore likely that the GPI-APs$^-$ clones with a frequency of less than 0.25% reflect hematopoiesis maintained by a single HSC. It is clear from our studies that most of these small clones contain only limited lineage cells. Even in the case of larger clones, for example, clones of 1%–3% chimerism that might be maintained more than two HSCs, the majority (81%) are non-full-lineage clones. Collectively, these results indicate that most individual human HSCs only give rise to a limited range of hematopoietic progeny.

A Model for the Hematopoietic Microenvironment to Explain the Production of Limited Cell Lineages from a HSC

A cogent explanation for this phenomenon may have important implications for normal hematopoiesis. We

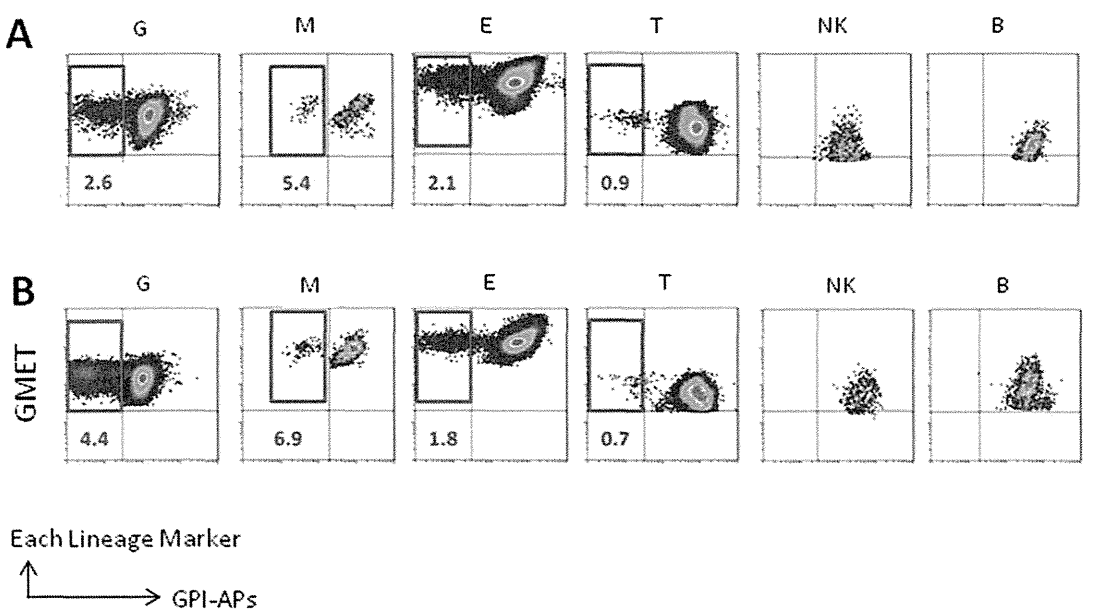

Figure 3. The lineage combination pattern of GPI-APs$^-$ cells was same at the first sampling **(A)** and after 6 months **(B)**. Abbreviation: GPI-APs, glycosylphosphatidylinositol-anchored proteins.

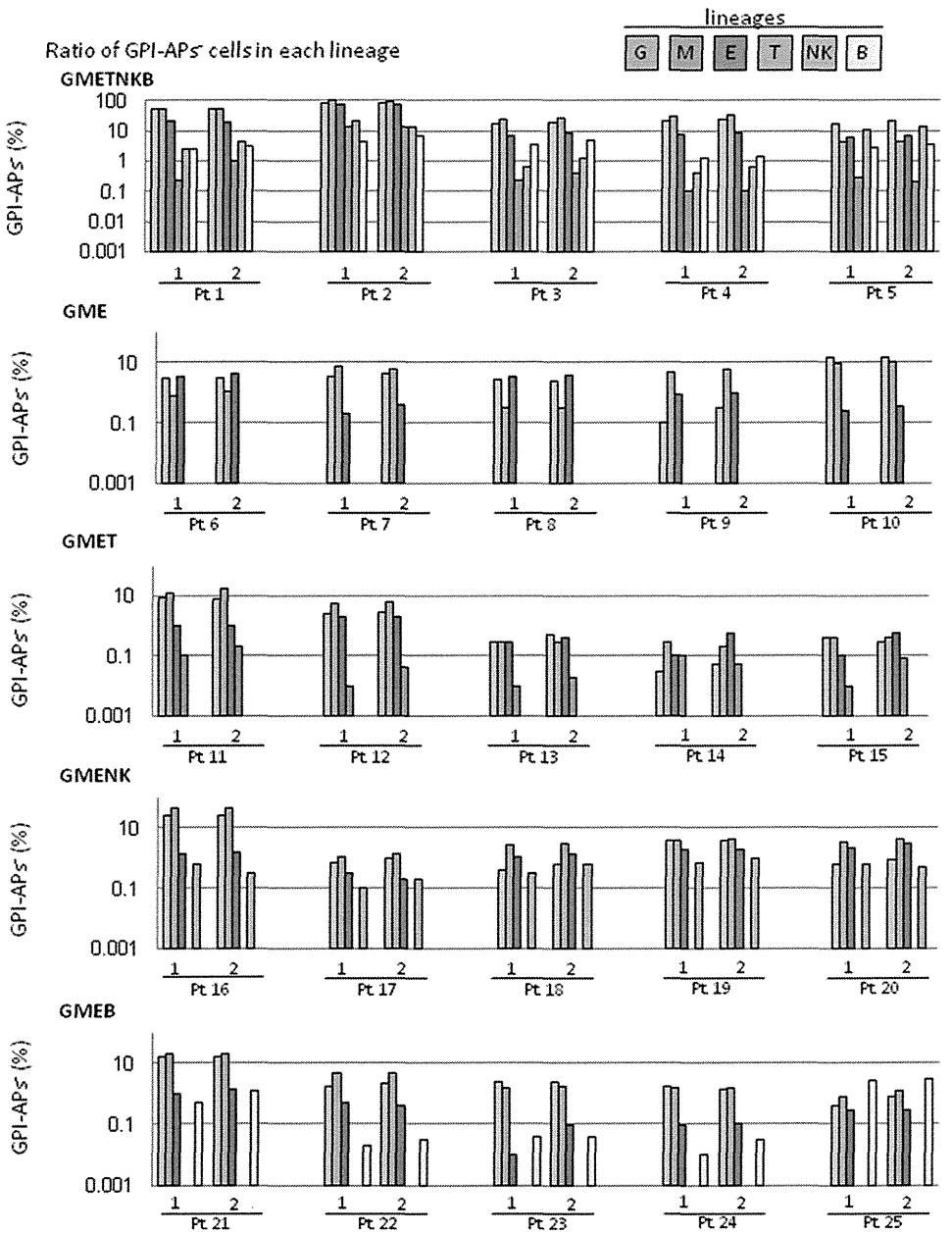

Figure 4. The combination of GPI-APs$^-$ lineage as well as the proportion of GPI-APs$^-$ cells in peripheral blood (PB) persists over a long period. GPI-APs$^-$ cells were analyzed in PB of 250 patients twice at intervals ranging 6–18 months. The numbers 1 and 2 refer to the first and second analysis. In all cases, GPI-APs$^-$ cells were detected in the same lineages in both analyses. Among them, 25 cases (five for each type of lineage combination) are shown. Bars represent the proportion of GPI-APs$^-$ cells in each lineage in PB. Abbreviations: GPI-APs, glycosylphosphatidylinositol-anchored proteins; GMET, Granulocyte, Monocyte, Erythrocyte, T cell.

considered several possible explanations such as: (a) the limited lineage spectrum of progeny cells may reflect the presence of progenitors with equally limited potential, (b) HSCs are intrinsically heterogeneous in terms of developmental potential, and (c) BM environment is heterogeneous in its ability to support the differentiation of distinct lineages. However, as will be discussed later, these cases seemed quite unlikely. Instead of above ideas, we came to think that the unexpected production of limited cell lineages by HSCs may be explained by assuming the presence of mosaic-like hematopoietic environments that can differently support the "commitment" of early multipotent progenitors to a certain lineage.

We attempted to test this idea by modeling and simulation. For simplicity, granulocytes and monocytes are placed into the myeloid lineage while T and NK cells are placed into the T lineage, consequently all lineages being classified into M, E, T, and B lineages. The clinically observed data for chimerism ratio and detected lineages shown in Figure 2A are replotted in Figure 6A. For cases where the proportion of GPI-APs$^-$ clones is between 0.3% and 3% (representing typical size clones), the frequencies of different lineage combinations are shown in Figure 6B.

We assume that a self-renewing HSC is located in a particular location in BM and that uncommitted progenitors derived from this HSC can reach to a certain defined area

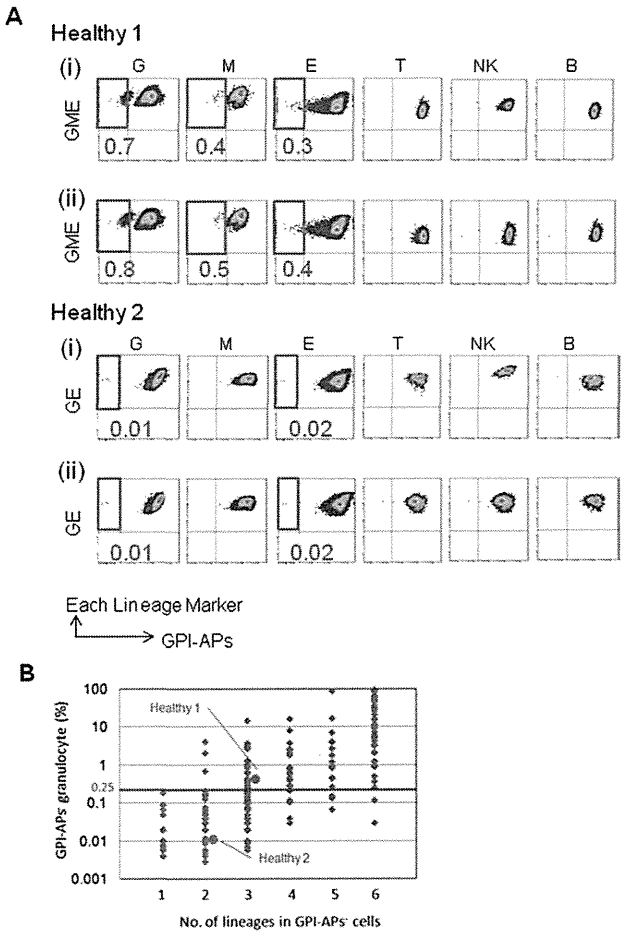

Figure 5. GPI-APs$^-$ cells in healthy individuals. **(A):** Two healthy individuals (healthy 1 and healthy 2) showed GPI-APs$^-$ cells in the same lineage combination pattern at the first sampling (i) and 13 and 7 months after the first sampling (ii), respectively. **(B):** The percentage of GPI-APs$^-$ granulocytes in the two healthy individuals is shown as closed circle in red. ◆, aplastic anemia and myelodysplastic syndrome cases are shown in Figure 2A. Abbreviations: GPI-APs, glycosylphosphatidylinositol-anchored proteins; GMET, Granulocyte, Monocyte, Erythrocyte, T cell.

(Fig. 6C), which we term here the "commitment sphere" (see also Supporting Information Note for detailed information). If the BM microenvironment is mosaic in terms of function in inducing the commitment of progenitors toward a certain lineage, and the size of such mosaic is as large as commitment sphere, then production of progenitors of limited lineages can occur.

In our model, it is critical to determine how the mosaic-like environment is distributed in BM. To this end, we comprehensively examined 112 kinds of mosaic patterns, varying grains of area ratios among commitment areas supporting M, E, B, and T. The strategy to generate the patterns is summarized in the Supporting Information Note. For each mosaic pattern out of 112 variants, we simulated that a single randomly located HSC in certain type of mosaic environment undergoes a certain round of cell division and then undergo commitment according to the place they are located. After commitment, cells further make proliferation and finally terminal differentiation to form mature blood cells. For simplicity, the number of cell division before and after commitment is set as 5 and 5, respectively, in the simulation. We then investigated which cell lineages appeared, counting the number of cells belonging to each lineage. A total of 100 clones were simulated for each mosaic pattern. We found that simulation based on 17 mosaic patterns resulted in histograms similar to the clinical data. Figure 6C shows a representative mosaic among them, and Figure 6D shows the histogram for the results of simulations in which a total of 256 of randomly located HSCs gave rise to hematopoietic colonies in the mosaic pattern shown in Figure 6C, which recapitulate the clinical results (Fig. 6B). We also performed simulations of many virtual HSCs in the same mosaic environment while changing clone size (i.e., changing the cell division times before and after commitment, e.g., 3-3, 4-4, 5-5, 6-6, 7-7, resulting in the change in the size of the commitment sphere and the colony of mature cells). The relationship between clone size and number of lineages in each clone was then plotted in Figure 6E, which looks quite similar to Figure 6A. Thus, these simulations may have provided a reasonable explanation for the observed in vivo findings.

In the simulation, we assumed that T/NK cell progenitors and B cell progenitors are generated in distinct sites. If the induction site for T/NK cell progenitors is assumed to completely overlap or to be included as a part of B cell progenitor induction site (Fig. 7A, 7B), our simulation predicts that "MET"-type clones would hardly be generated (Fig. 7C, 7D), which is not the actual case. Therefore, our in vivo findings together with the results of simulation strongly suggest that T/NK cell progenitors are produced in a different site from the one where B cell progenitors are produced.

Discussion

In this study, by flow cytometrically detecting GPI-APs$^-$ cells in major six blood lineages, we have succeeded in visualizing the dynamics of individual HSCs in BM failure patients. The results strongly suggest that most individual human HSCs only give rise to a limited range of hematopoietic progeny even in regular hematopoiesis.

We thought that we should provide a reasonable explanation for this unexpected finding, that is, the detection of GPI-APs$^-$ cells in the limited lineages over long period. Before we reach to our model, we have considered several possibilities to explain this finding, as briefly mentioned in Result. Here, we will discuss these possibilities, (a), (b), and (c).

(a). One possibility is that the limited lineage spectrum of progeny cells may reflect the presence of progenitors with equally limited potential. Indeed, in contrast to classic models of hematopoiesis, which assume the early segregation of HSCs to myelo-erythroid lineage and lymphoid lineage, some recent revised models of both mouse and human hematopoiesis have proposed that myeloid lineages are also derived from lymphoid branches [21, 22]. However, implications of these models in this study seem unlikely, since, as mentioned earlier, it is clear that most cases represent activities of self-renewing HSCs.

(b). Another simple explanation might be that HSCs are intrinsically heterogeneous in terms of developmental potential. Recent studies have shown such heterogeneity in murine HSCs, some being prone to produce myeloid cells while others to produce lymphoid cells [23–28]. However, it seems quite unlikely that HSCs intrinsically have as many as 16 different subtypes as shown in Supporting Information Table S1.

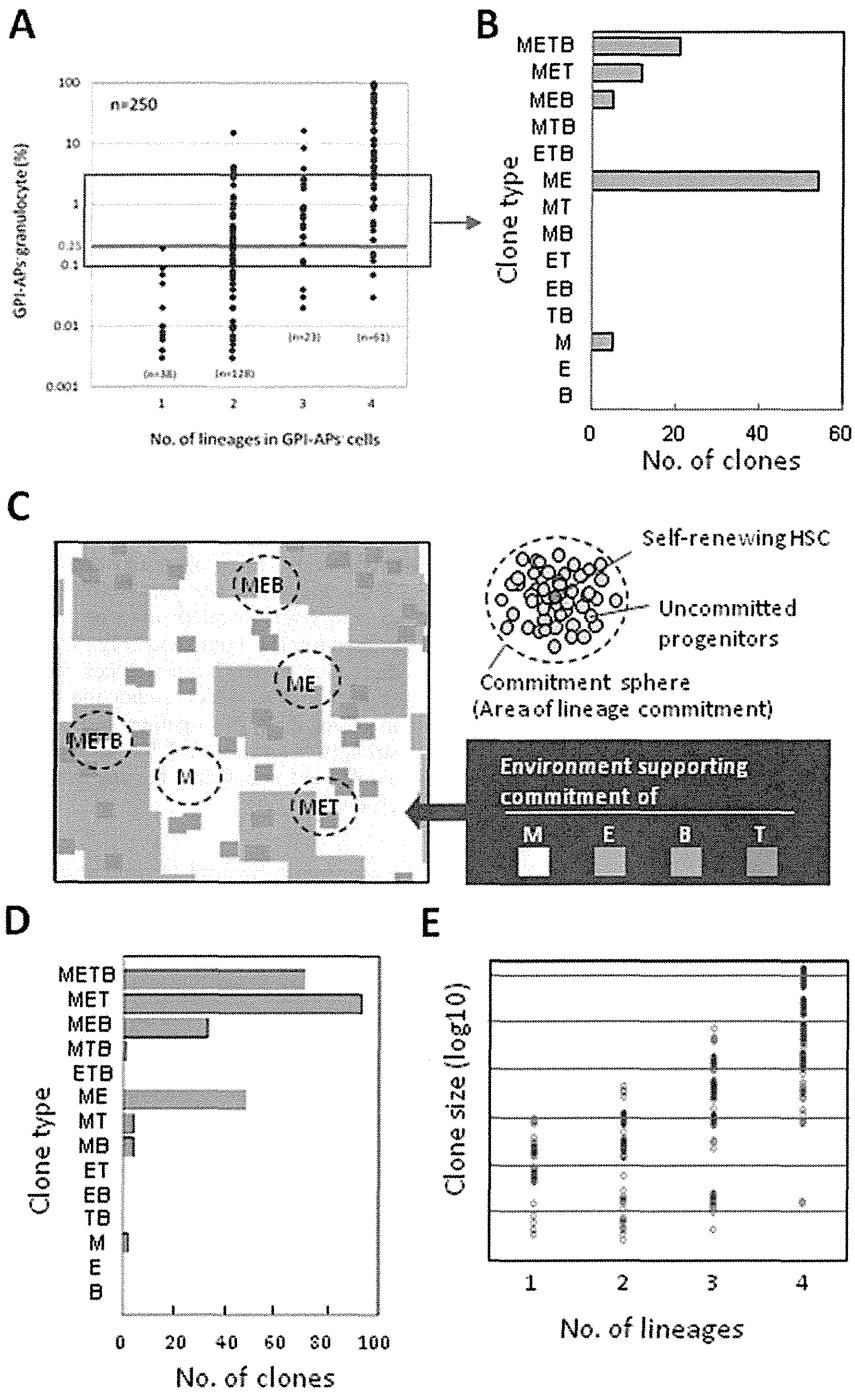

Figure 6. Simulation of hematopoietic stem cell (HSC) differentiation in a model assuming a mosaic environment for the commitment of primitive progenitors recapitulates the clinical observation. **(A):** The percentage of GPI-APs$^-$ granulocytes versus the number of cell lineages in individual patients. Data from Figure 2A were replotted in a setting where granulocytes and monocytes were placed in the myeloid lineage and T and NK cell lineages in the T-cell lineage. A red line for 0.25% stands for the expected value for an average size of a single HSC clone. **(B):** Frequency of clone types among cases where the percentage of GPI-APs$^-$ granulocytes is between 0.3% and 3%. **(C):** A model assuming that the bone marrow microenvironment is heterogeneous in supporting the commitment of progenitors. A certain range where the commitment of progenitors mainly occurs (with a probability of >97%) is termed the commitment sphere (see Supporting Information Note for detailed information). Areas colored by beige, pink, light green, or blue represent the environment supporting commitment only toward M, E, T, or B, respectively. If a HSC happens to reside in a location in which the commitment sphere contains only M and E regions, then this HSC can eventually produce only M and E cells, even if committed progenitors expand enormously and become widely scattered. The depicted simulation goes as follows: a virtual HSC undergoes several cell divisions at fixed intervals while randomly migrating. The uncommitted progenitors then undergo a fate decision based on their ultimate location in the commitment sphere. Committed progenitors can also randomly move around but can proliferate only in the lineage specific supporting environment. After several additional fixed time cell divisions as committed progenitors, cells become mature and lineage restricted. **(D):** One example illustrating the frequency of clone types simulated as shown in (C). A total of 100 virtual HSCs were simulated to form hematopoietic clones, and numbers of the resulting clone types are illustrated (Supporting Information movies 1–5). **(E):** Simulation of individual HCSs for size and number of progeny lineages. The simulation well recapitulated the clinical observations shown in (A). Abbreviation: GPI-APs, glycosylphosphatidylinositol-anchored proteins.

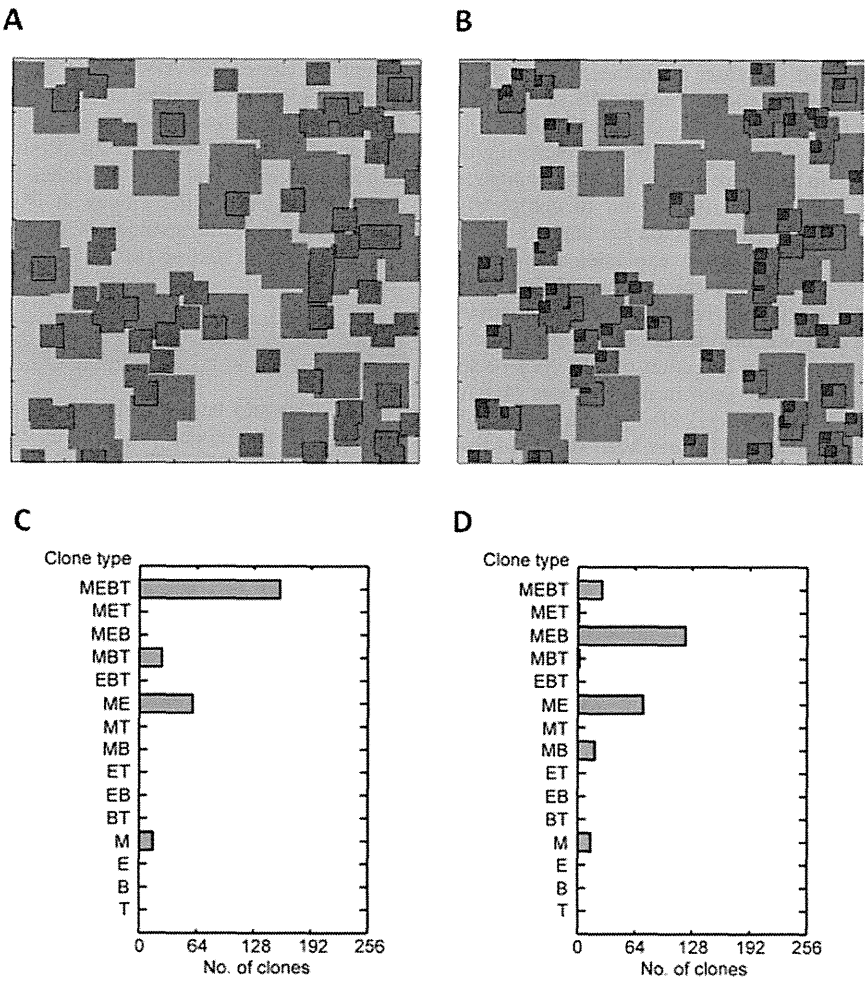

Figure 7. Alternative conditions for induction sites to T and B cell lineages. Illustration of a mosaic pattern in a case where the induction site to the T lineage completely **(A)** or partially **(B)** overlaps with the B lineage (i.e., green area is for both T and B in (A), while blue area is for T and green area is for B in (B)). **(C, D):** Histograms calculated from Panel A (C) or Panel B (D).

(c). It is also possible that the BM environment is heterogeneous in its ability to support the differentiation of distinct lineages. However, this is also quite unlikely. Provided that 400 stem cells contribute to whole hematopoiesis [1, 2] containing 18×10^{11} hematopoietic cells [29] in a total of approximately 1 kg active BM mass [30], the size of the hematopoietic site of one clone maintained by a single HSC in BM could be several cm^3, which may contain on the order of 10^9 hematopoietic cells and a comparable number of stromal cells. It is thus difficult to conceive that such large area contains only limited types of microenvironments.

Thus, we came to think that the above three explanations were quite unlikely. We then came to propose a reasonable model as an explanation of this phenomenon. This model assumes that the microenvironment of BM is mosaic in inducing the commitment of progenitors to distinct lineages. If the size of area where uncommitted progenitors derived from one HSC can reach (commitment sphere in Fig. 6C) is similar to the size of mosaic compartments, production of limited lineage cells can occur. We named our model "mosaic commitment-inducing microenvironment model." This idea on first viewing may sound similar to the idea mentioned above in (c), but clearly different in that our model focuses on only commitment-inducing function of microenvironment and thus the size of mosaic area is much smaller. In this context, our model is also distinct from the classic idea of "hematopoietic inductive microenvironment (HIM)" [31], which is close to the idea mentioned above in (c).

To test whether our model can explain the in vivo findings, we applied a computer simulation approach, and simulations based on this model nicely recapitulated the observed in vivo findings. We emphasize here that we do not claim that our in vivo findings indicate the presence of mosaic commitment-inducing microenvironment in BM, but just propose a novel model that can explain the finding which otherwise is difficult to explain.

We recognize that the issue of whether the dynamics of HSCs observed in this study represents normal hematopoiesis must be critically discussed. Since the stable production of limited lineages was observed in milder cases of AA patients similarly to more severe cases (Fig. 2B), it is likely that these observed dynamics represent normal hematopoiesis. Detection of stable GPI-APs$^-$ clones producing limited lineages in healthy volunteers further supports this notion (Fig. 5).

Nevertheless, here we will make discussion on the issue whether we are making some overestimation or

underestimation in the interpretation of data in AA and MDS cases. Our findings can be summarized as follows: (a) a single HSC gives rise to a limited spectrum of lineage cells and (b) HSCs stably and continuously produce blood cells by years.

As for the finding (a), the possibility could exist that GPI-APs$^-$ HSCs or progenitors have some defect in their migration potential, resulting in a failure to produce the complete spectrum of lineages. Although it is difficult to completely rule out this possibility, so far no published findings are available that support it. Another possible explanation could be that the HSCs in AA or MDS patients are already defective in developmental potential, or that the hematopoietic microenvironments in these patients are disorganized. However, these may not be critical factors, since detection of GPI-APs$^-$ cells of limited lineages was similarly seen in milder cases of AA, and also in healthy volunteers (Figs. 2B, 5). AA and MDS may result from various causes, and it has been supposed that a certain proportion of cases are primarily caused by the impaired function of microenvironment. However, it is likely that in most cases in this study the microenvironment itself is largely normal, because all the patients are bearing GPI-APs$^-$ cells, which is a sign to show that immunological pathophysiology is the main cause of the disease. It can also be noted that most AA patients who undergo allogeneic BM transplantation achieve complete hematologic recovery despite the fact that BM stromal cells are not transplantable [32], indicating that the hematopoietic microenvironments in AA patients are not impaired. Another possibility to be discussed is that the immunological reaction against GPI-APs$^-$ HSCs may affect their blood cell formation, since AA and MDS cases bearing GPI-APs$^-$ cells are thought to be caused by such autoimmune activities. However, such effect cannot be essential, since GPI-APs$^-$ cells are usually out of the target of immune cells, and the autoimmune activities in patients tested in this study have been virtually negligible, judging from the fact that the clone sizes of GPI-APs$^-$ cells in all patients scarcely changed during the observation periods.

We used antibody for CD55, CD59, or CD48 to positively stain GPI-AP expressing cells instead of FLAER that directly stain GPI-APs. In calibration experiments, we have seen that both methods virtually made no difference (data not shown). We note here that our approach could result in the overestimation of the presence of GPI-APs$^-$ cells compared with the FLAER method, since FLAER can cover all GPI-APs. However, such overestimation seems to occur at a very low frequency, and moreover, it will never cause the underestimation for the presence of GPI-APs$^-$ cells.

Finding (b) seems to fit well with the expected dynamics of HSCs. However, this finding could result from an overestimation. Since patients have some BM failure, the total HSC number may be more or less reduced. In such a less competitive situation, it could be that the active HSCs have a better chance to continue hematopoiesis. In addition, GPI-APs$^-$ cells may have some survival advantage over normal blood cells in patients because GPI-APs$^-$ cells may be less sensitive to immunological attacks than GPI-APs$^+$ cells [33]. However, in fact, the combination of GPI-APs$^-$ lineage as well as the proportion of GPI-APs$^-$ cells in PB persisted over a long period as it is, indicating that most of clones do not have an obvious dominance against other clones. It is also important to note that any possible overestimation in HSC longevity does not call into question finding (a).

Conclusion

Finally, it should be discussed whether such heterogeneity as proposed in our model can actually be observed in the BM environment. Heterogeneity of stromal environment has been pointed out in early studies for example based on the findings of preferential generation of erythroid or granulocytic cells in spleen and BM, respectively [31]. A recent study has suggested the presence of a microenvironment that selectively supports B cell development in murine BM [34]. This then leads to the question of how large is the commitment sphere and mosaic fragments of the BM environment? We do not have any data concerning the actual size of the commitment sphere or compartments of mosaic environments, but would suggest that the relative size of these two may be similar to each other. Thus, each piece of the mosaic could be very small, containing only a few stromal cells. We hope that our present report and speculative model will facilitate further study on the distinct niches in BM environment.

Acknowledgments

This study was supported by Grant-in-Aids for Scientific Research from the Ministry of Education, Culture, Sports, Science and Technology of Japan (KAKENHI No. 21390291, http://www.e-rad.go.jp/) and a Grant-in-Aids from the Ministry of Health, Labor and Welfare of Japan. The calculations were performed using the RIKEN Integrated Cluster of Clusters (RICC) facility.

Disclosure of Potential Conflicts of Interest

The authors indicate no potential conflicts of interest.

References

1 Buescher ES, Alling DW, Gallin JI. Use of an X-linked human neutrophil marker to estimate timing of lyonization and size of the dividing stem cell pool. J Clin Invest 1985;76:1581–1584.

2 Traulsen A, Pacheco JM, Luzzatto L et al. Somatic mutations and the hierarchy of hematopoiesis. Bioessays 2010;32:1003–1008.

3 Wang H, Chuhjo T, Yasue S et al. Clinical significance of a minor population of paroxysmal nocturnal hemoglobinuria-type cells in bone marrow failure syndrome. Blood 2002;100:3897–3902.

4 Nishimura J, Inoue N, Wada H et al. A patient with paroxysmal nocturnal hemoglobinuria bearing four independent PIG-A mutant clones. Blood 1997;89:3470–3476.

5 Rosti V, Tremml G, Soares V et al. Murine embryonic stem cells without pig-a gene activity are competent for hematopoiesis with the PNH phenotype but not for clonal expansion. J Clin Invest 1997;100:1028–1036.

6 Maciejewski JP, Sloand EM, Sato T et al. Impaired hematopoiesis in paroxysmal nocturnal hemoglobinuria/aplastic anemia is not associated with a selective proliferative defect in the glycosylphosphatidylinositol-anchored protein-deficient clone. Blood 1997;89:1173–1181.

7 Araten DJ, Luzzatto L. The mutation rate in PIG-A is normal in patients with paroxysmal nocturnal hemoglobinuria (PNH). Blood 2006;108:734–736.

8 Traulsen A, Pacheco JM, Dingli D. On the origin of multiple mutant clones in paroxysmal nocturnal hemoglobinuria. Stem Cells 2007;25:3081–3084.